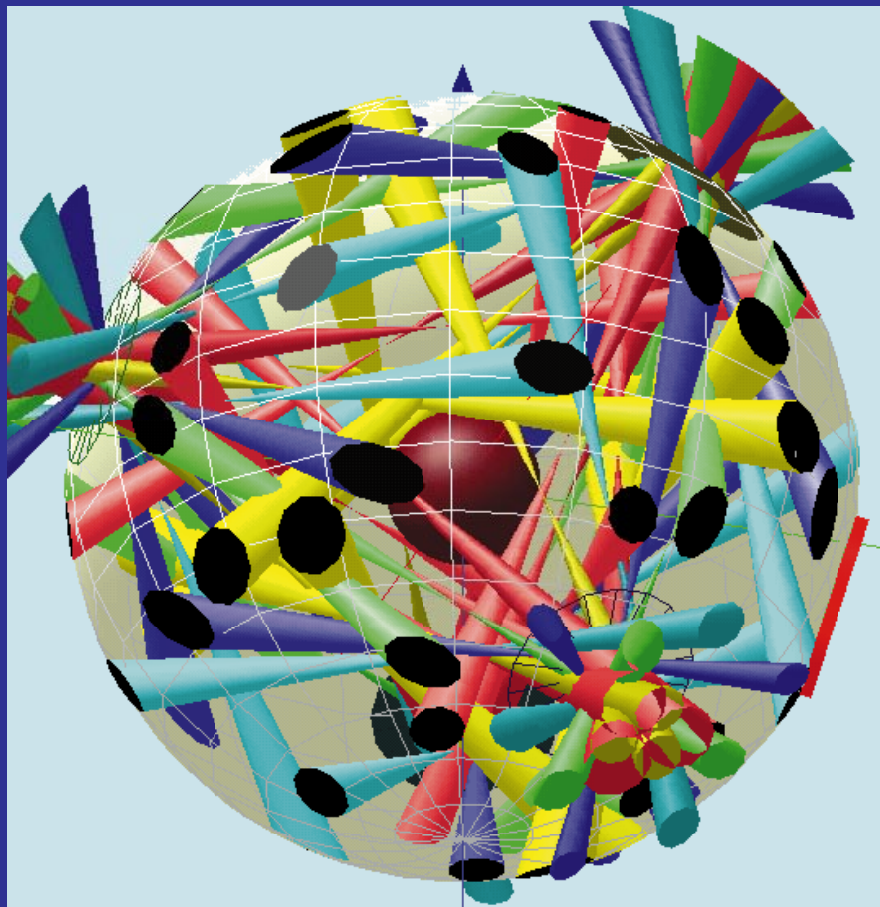


*Tetrahedral Hohlräum  
High-Convergence Implosion  
Experiments on Omega  
ID6-FY99*

*March 1 – March 5, 1998*



# High-convergence implosions in tetrahedral hohlraums shot plan (ID6-March 1-5, 1999)

<b>Introduction and background</b>	<b>2</b>
<b>Objectives</b>	<b>3</b>
<b>Experimental Plan</b>	<b>3</b>
Target description	3
Pulse shape	3
Alignment choice	4
Pointing scheme	5
<b>Beam pointing</b>	<b>7</b>
LEH positions	8
Beams in each beam cone	8
Beam alignment	10
Target alignment	11
<b>Experiments to be performed</b>	<b>11</b>
Pointing sphere targets	11
Double shell implosion targets	12
High-convergence single-shell implosion targets	13
Metrology of high-convergence single-shell targets	14
<b>References</b>	<b>14</b>
<b>Attachments</b>	<b>16</b>

*This document is intended to give an overview of this experimental campaign. Where information conflicts with experimental configurations submitted by official methods, those configurations take precedence. Contact the Principal Investigator prior to making any changes in the configuration to accommodate conflicts of information based on this document.*

*This document was produced by the Los Alamos National Laboratory under the auspices of the United States Department of Energy under contract no. W-7405-ENG-36.*

## Introduction and background

The utility of the Omega laser facility for indirect-drive inertial confinement fusion experiments has been irrefutably demonstrated [1-3]. Experiments have demonstrated that cylindrical hohlraums using up to 40 of the 60 Omega beams can be used to produce symmetric implosions with shapes predictable by existing ICF codes. [2]

Experiments have also been performed [4,5] that utilize spherical hohlraums with a tetrahedral arrangement of laser entrance holes [6,7], also known as “tetrahedral hohlraums.” These experiments allow the use of all 60 Omega beams to drive implosions, and have potential symmetry advantages over cylindrical hohlraums. In the first set of experiments [8], x-ray drive and implosion symmetry and performance were measured using spherical hohlraums with 2300- $\mu\text{m}$  inside diameter (scale-1) with 1 ns sq and shaped laser drives, and 2800- $\mu\text{m}$  inside diameter (scale-1.2) with 1 ns sq laser drive. Implosion images obtained through a laser entrance (LEH) hole showed a distinctive  $m=3$  component aligned with the LEHs.

A follow-up set of experiments utilized scale-1.2 hohlraums with reduced laser entrance hole diameters and shaped laser pulses. The combination created implosion images with almost no  $m=3$  component in the shape. While fully-integrated three-dimensional calculations of the symmetry from an inherently three-dimensional experiment such as this are not available, simpler calculations indicate that these hohlraums produce a radiation drive with greatly reduced time-dependent asymmetry as compared to cylindrical hohlraums. Therefore, this configuration has the potential to allow implosion hydrodynamics experiments that do not have the complication of time-dependent drive asymmetry affecting the interpretation of the data.

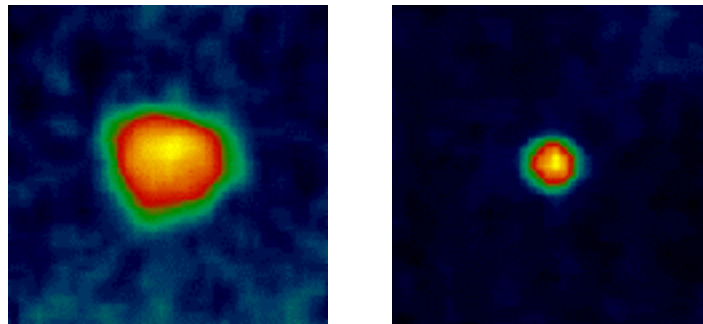


Figure 1: In the first set of tetrahedral experiments, implosion images contained a significant  $m=3$  component (left), while larger hohlraums, smaller LEHs, and longer pulse shape reduced the  $m=3$  component to negligible levels in a follow-up campaign (right).

## Objectives

In this experiment, we will investigate the behavior of high convergence capsule implosions in tetrahedral hohlraums:

1. Double shell implosions will investigate techniques to improve performance over the historical few percent of clean 1-D calculational yields at high convergence, by varying the ablator material and the inner capsule composition;
2. Single shell implosions will investigate techniques to improve performance over the historically degraded level at several convergence ratios by doping the outer ablator and will compare nominally identical capsule designs to the recent LLNL results from Omega in cylindrical hohlraums.

During this set of experiments, the Los Alamos bangtime detection system will be made operational.

## Experimental Plan

### *Target description*

The targets will consist of thin-wall scale-1.2 spherical hohlraums (inside diameter of 2800  $\mu\text{m}$ ), with four 700- $\mu\text{m}$  diameter laser entrance holes arranged in a tetrahedral pattern. The wall will consist of 100  $\mu\text{m}$  of epoxy (by weight, 74.4% C, 7.1% H, 18.1% O, 0.4% N; by atom, 42.8% C, 49.1% H, 18.1% O, 0.2% N; specific density =1.15) with a 2- $\mu\text{m}$  gold lining.

The hohlraums will either contain a "double-shell" capsule or a high-convergence single shell capsule with a nominal outside diameter of 550  $\mu\text{m}$ . The double shell capsules will have a 36 atm fill of either DD(3 ea.) or DT(6 ea.). All single shell implosions are DD filled with varying pressures. The hohlraums will be aligned with one LEH in line with TIM2 for capsule imaging.

### *Pulse shape*

Two different pulse shapes will be used during the tetrahedral hohlraum campaign. The first will be a 1 ns flat top laser pulse.

The second laser pulse shape will be similar to that referred to on Omega as pulse shape 26 (equivalent to NOVA PS26). This is a laser pulse with a duration of approximately 2.6 ns, consisting of a 1.0 ns foot, followed by a ramp up to a maximum at about 1.6 ns, a 1 ns flattop, and a subsequent fall. The contrast of this pulse shape is approximately 5 to 1.

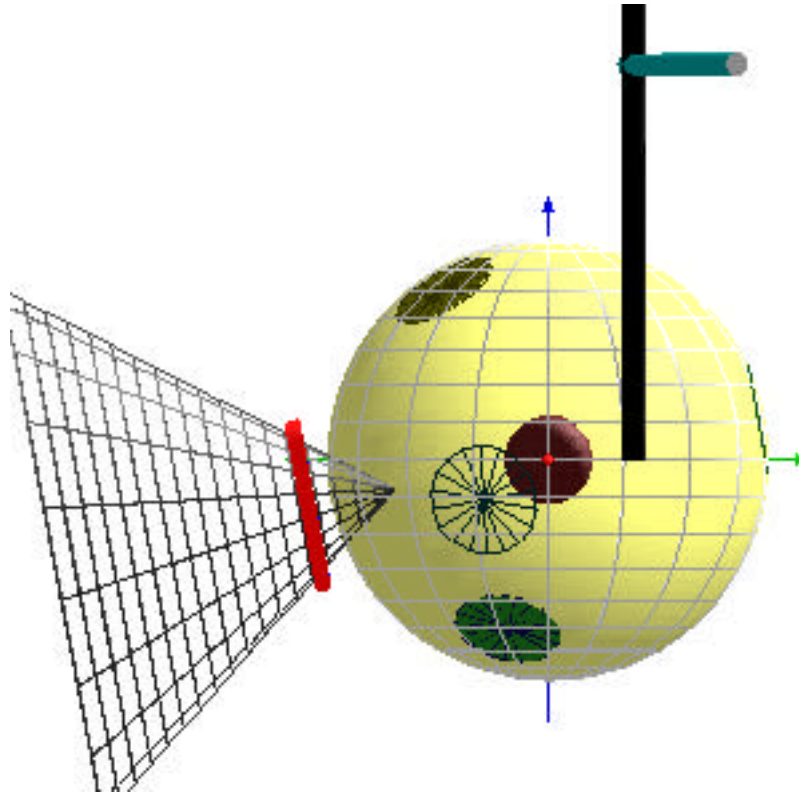


Figure 2: View of tetrahedral hohlraum from the North. The conical shield shown in the figure will not be used in the present experiments.

### **Alignment choice**

On Omega, each of the hexagonal ports has six other hexagonal ports located  $109.47^\circ$  away, the angle for tetrahedral symmetry. These six consist of two groups of three ports which, in turn, are made up of ports  $109.47^\circ$  from each other. Each port, along with one of the groups of three, defines one tetrahedral alignment. Since there are 20 hexagonal ports, and each alignment uses four of the ports, there are ten unique tetrahedral alignments on Omega (Table 1). The choice of two ports  $109.47^\circ$  apart uniquely defines the alignment.

For the set of experiments performed in ID6-March 1-5, 1999, the 4-7 configuration will be used. This orientation was chosen due to the availability of certain diagnostics, the most important being TIM 2, which will hold either XRFC4 or LANL's QXI to view the capsule through LEH B centered on H7. In addition, Dante will view the hohlraum wall through LEH D centered on H20 at a  $42^\circ$  angle, and LEH D will be monitored with a soft-x-ray framing camera (SXRFC3) from TIM 6. Either XRFC3 or LANL GXI-T will view the laser spots from TIM 1.

Designation	Ports			
1-8	H1	H8	H14	H17
1-9	H1	H9	H11	H18
2-9	H2	H9	H13	H16
2-10	H2	H10	H15	H17
3-6	H3	H6	H14	H16
3-10	H3	H10	H12	H20
4-6	H4	H6	H11	H19
4-7	H4	H7	H13	H20
5-7	H5	H7	H15	H18
5-8	H5	H8	H12	H19

Table 1: Sets of hexagonal ports on Omega that constitute unique tetrahedrally symmetric orientations

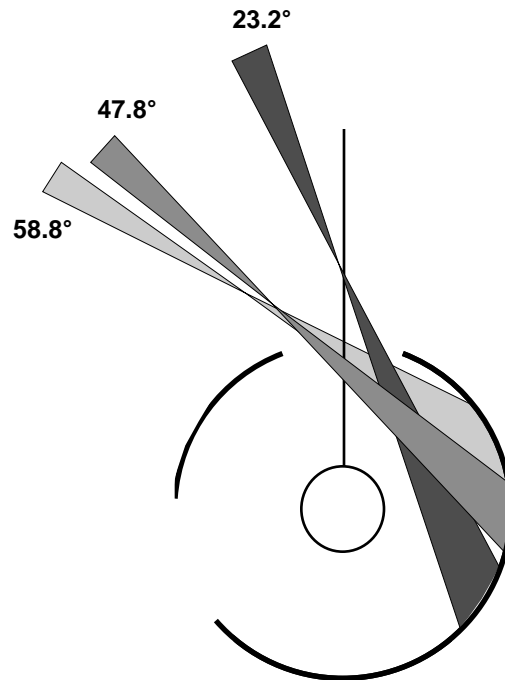


Figure 3: Illustration of the entrance angles of the beams in tetrahedral illumination of spherical Omega hohlraums.

### Pointing scheme

The choice of beam pointing [9] is made based on having all 60 beams enter the hohlraum, not having the beams strike the capsule or one of the other laser entrance holes, and minimizing the flux asymmetries created due to the laser entrance holes. By necessity, the beams are pointed in such a way that they do not cross the axis of the laser entrance hole.

The beams can be divided into three cones according to their angle with respect to the ray from target chamber center through the laser entrance hole.

In order of increasing angle, they are cone 1 ( $23.2^\circ$ ), cone 2 ( $47.8^\circ$ ), and cone 3 ( $58.8^\circ$ ). Cones 1 and 2 contain 6 beams each, and cone 3 contains 3 beams.

Beam cones 1 and 2 can be further divided into cones of 3 beams each according to whether or not they come close to laser entrance holes when they reach the far side of the hohlraum. Beam cones 1a and 2a come close, while cones 1b and 2b fall between laser entrance holes. Thus, pointing numbers can be derived for five different beam cones of 3 beam each per laser entrance hole.

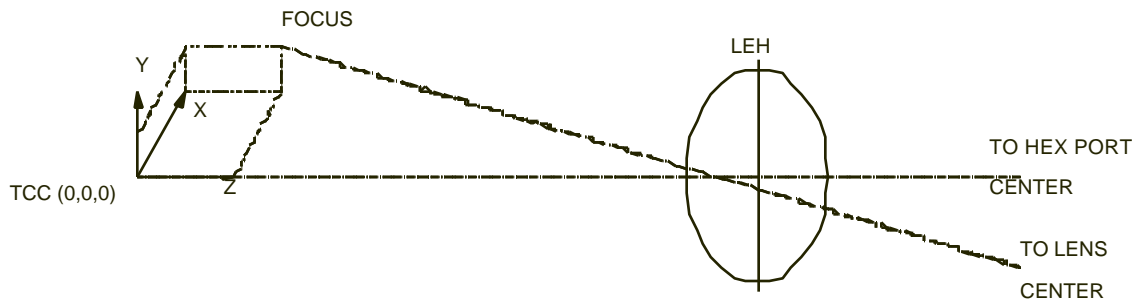


Figure 4: Coordinate system used in determining pointing for the beam cones in Omega tetrahedral hohlraums. Note that this drawing replaces the drawing in previous IDX preshot reports, which was incorrect. This drawing is the correct geometry.

Beam Cone	X	Y	Z
1A	525	-45	256
1B	370	-50	700
2A	455	20	1035
2B	375	-170	1000
3	110	-50	1278

Table 2: Coordinates for the scale-1.2 tetrahedral pointing used in ID6-March 1-5, 1999.

The pointing is specified in a coordinate system in which the origin is at target chamber center. The z axis is along the ray from TCC through the center of the laser entrance hole. This ray and the ray from TCC to the center of the

lens for the beam in question form a plane. The x axis lies in this plane and is perpendicular to the z axis. The y axis is perpendicular to the x and z axes and the three form a right-handed coordinate system. The pointing of each of the beams is determined by the position of best focus in this x, y, z coordinate system. From these values, the offsets for the beams can be determined.

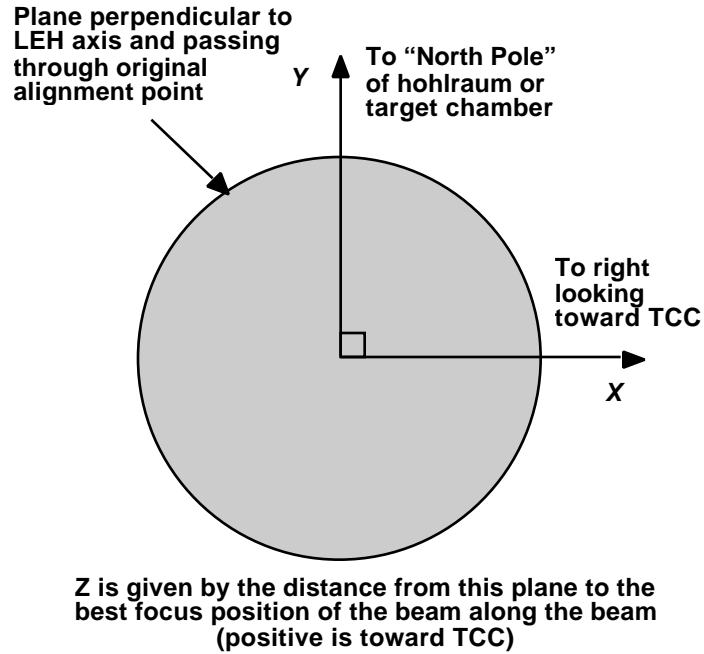


Figure 5: Definition of beam offsets used by LLE.

## Beam pointing

Hohlraum orientation: H4-H7-H13-H20



**LEH positions**

LEH	Port	Theta	Phi
LEH A:	H4	37.4°	234°
LEH B:	H7	79.2°	90°
LEH C:	H13	100.8°	342°
LEH D:	H20	142.6°	198°

**Beams in each beam cone**

Cone A1a:	55, 46, 48	Cone C1a:	39, 16, 37
Cone A1b:	61, 52, 26	Cone C1b:	21, 35, 15
Cone A2a:	65, 17, 41	Cone C2a:	12, 34, 10
Cone A2b:	56, 60, 33	Cone C2b:	29, 27, 28
Cone A3:	22, 36, 40	Cone C3:	38, 31, 23
Cone B1a:	59, 18, 13	Cone D1a:	45, 44, 54
Cone B1b:	67, 66, 24	Cone D1b:	62, 64, 51
Cone B2a:	47, 14, 11	Cone D2a:	25, 42, 43
Cone B2b:	69, 68, 32	Cone D2b:	57, 19, 63
Cone B3:	50, 20, 58	Cone D3:	53, 49, 30

## 0 Tetrahedral Pointing Parameters—Nominal (No Backlight)

config: 407				unit hole vector -- kk z			Sphere intercept 1400 μm from TCC			LEH center 1355.54 μm from TCC		
LEH	Port	Theta	Phi	X	Y	Z	X	Y	Z	X	Y	Z
A	4	37.38	234	-0.357	-0.491	0.795	-500	-688	1113	-484	-666	1077
B	7	79.19	90	0.000	0.982	0.188	0	1375	263	0	1331	254
C	13	100.8	342	0.934	-0.304	-0.188	1308	-425	-263	1266	-411	-254
D	20	142.6	198	-0.577	-0.188	-0.795	-808	-263	-1113	-783	-254	-1077

"Try4" positions for Scale-1.2 pointing

Cone	Angle	R(LEH) 350		
		X	Y	Z
kk offsets in μm				
1A	23.20	525	-45	256
1B	23.20	370	-50	700
2A	47.83	455	20	1035
2B	47.83	375	-170	1000
3	58.79	110	-50	1278

R retro	RRRmax	2381	3/16" BB
1356	171	1984	5/32" BB

2/16/99 15:54		Beam	Beam	Beam	Focus wrt TCC	Retro Dead Recon Offset			Check Sphere					
LEH	Cone	Beam	Theta	Phi	ZZ	X	Y	Z	XXX	YYY	ZZZ	theta	phi	ZZZZ
A	1A	55	42.0	198.0		297	-479	159	51	-48	1197	38.8	-135.9	-671
A	1A	46	21.4	270.0		-547	-203	-49	-67	-20	1197	31.6	-121.7	-671
A	1A	48	58.9	246.1		-24	305	500	16	68	1197	42.4	-120.2	-671
A	1B	61	21.4	198.0		-278	-655	351	6	-102	714	34.1	-133.1	-674
A	1B	52	58.9	221.9		66	-271	743	85	56	714	42.6	-127.5	-674
A	1B	26	42.0	270.0		-537	-105	575	-91	45	714	36.0	-117.4	-674
A	2A	65	58.9	174.1		15	-752	845	100	24	478	39.9	-150.0	-834
A	2A	17	21.4	342.0		-720	-658	573	-29	-98	478	25.3	-108.1	-834
A	2A	41	81.2	257.5		-403	-115	1050	-70	75	478	51.0	-116.4	-834
A	2B	56	21.4	126.0		-528	-770	545	-159	-64	530	26.8	-154.8	-786
A	2B	60	81.2	210.5		27	-547	933	134	-106	530	55.2	-132.2	-786
A	2B	33	58.9	293.9		-569	-157	906	24	169	530	36.9	-95.4	-786
A	3_	22	21.4	54.0		-548	-669	949	-50	19	151	14.1	-131.9	-898
A	3_	36	81.2	282.5		-467	-523	1075	41	34	151	51.5	-99.0	-898
A	3_	40	81.2	185.5		-353	-691	1023	9	-53	151	53.4	-150.3	-898
B	1A	59	81.2	113.5		522	238	119	-51	48	1197	78.3	96.3	-671
B	1A	18	98.8	77.5		-324	173	456	67	20	1197	85.0	87.8	-671
B	1A	13	58.9	77.9		-198	343	-432	-16	-68	1197	74.4	85.9	-671
B	1B	67	98.8	102.5		160	624	463	-6	102	714	82.7	94.0	-674
B	1B	66	58.9	102.1		213	745	-170	-85	-56	714	74.0	91.1	-674
B	1B	24	81.2	66.5		-372	693	101	91	-45	714	80.9	84.9	-674
B	2A	47	81.2	138.5		454	1023	158	-100	-24	478	79.6	105.4	-834
B	2A	14	121.1	66.1		-196	939	598	29	98	478	92.3	82.5	-834
B	2A	11	42.0	54.0		-258	1087	-174	70	-75	478	66.2	81.8	-834
B	2B	69	121.1	113.9		26	905	591	159	64	530	92.6	102.6	-786
B	2B	68	42.0	126.0		343	1025	-36	-134	106	530	61.7	95.7	-786
B	2B	32	81.2	41.5		-369	1017	7	-24	-169	530	84.0	72.1	-786
B	3_	50	138.0	90.0		-50	1235	348	50	-19	151	102.5	91.5	-898
B	3_	20	58.9	30.1		-70	1274	143	-41	-34	151	69.8	67.7	-898
B	3_	58	58.9	149.9		120	1258	228	-9	53	151	67.2	111.0	-898

C	1A	39	121.1	354.1	265	-295	432	16	68	1197	105.6	-13.9	-671
C	1A	16	98.8	318.5	388	423	-119	51	-48	1197	101.7	-24.3	-671
C	1A	37	81.2	354.5	65	-361	-456	-67	-20	1197	95.0	-15.8	-671
C	1B	21	121.1	329.9	774	-28	170	85	56	714	106.0	-19.1	-674
C	1B	35	98.8	5.5	544	-568	-101	-91	45	714	99.1	-12.9	-674
C	1B	15	81.2	329.5	643	-41	-463	6	-102	714	97.3	-22.0	-674
C	2A	12	138.0	18.0	954	-582	174	-70	75	478	113.8	-9.8	-834
C	2A	34	98.8	293.5	1114	116	-158	100	24	478	100.4	-33.4	-834
C	2A	10	58.9	5.9	833	-476	-598	-29	-98	478	87.7	-10.5	-834
C	2B	29	138.0	306.0	1081	10	36	134	-106	530	118.3	-23.7	-786
C	2B	27	98.8	30.5	853	-665	-7	24	169	530	96.0	-0.1	-786
C	2B	28	58.9	318.1	869	-255	-591	-159	-64	530	87.4	-30.6	-786
C	3_	38	121.1	282.1	1233	-274	-228	9	-53	151	112.8	-39.0	-898
C	3_	31	42.0	342.0	1159	-429	-348	-50	19	151	77.5	-19.5	-898
C	3_	23	121.1	41.9	1190	-460	-143	41	34	151	110.2	4.3	-898
D	1A	45	158.6	162.0	-362	-458	49	67	20	1197	148.4	-166.3	-671
D	1A	44	121.1	185.9	282	-117	-500	-16	-68	1197	137.6	-167.8	-671
D	1A	54	138.0	234.0	-364	431	-159	-51	48	1197	141.2	-152.1	-671
D	1B	62	138.0	162.0	-266	-478	-575	91	-45	714	144.0	-170.6	-674
D	1B	64	158.6	234.0	-709	-62	-351	-6	102	714	145.9	-154.9	-674
D	1B	51	121.1	210.1	-238	146	-743	-85	-56	714	137.4	-160.5	-674
D	2A	25	158.6	90.0	-848	-481	-573	29	98	478	154.7	-179.9	-834
D	2A	42	98.8	174.5	-234	-348	-1050	70	-75	478	129.0	-171.6	-834
D	2A	43	121.1	257.9	-710	247	-845	-100	-24	478	140.1	-138.0	-834
D	2B	57	121.1	138.1	-325	-493	-906	-24	-169	530	143.1	167.4	-786
D	2B	19	158.6	306.0	-896	-264	-545	159	64	530	153.2	-133.2	-786
D	2B	63	98.8	221.5	-511	195	-933	-134	106	530	124.8	-155.8	-786
D	3_	53	98.8	149.5	-642	-282	-1075	-41	-34	151	128.5	171.0	-898
D	3_	49	98.8	246.5	-766	-122	-1023	-9	53	151	126.6	-137.7	-898
D	3_	30	158.6	18.0	-806	-314	-949	50	-19	151	165.9	-156.1	-898

Table 3: Detailed pointing for ID6.

### **Beam alignment**

The beams shall be aligned using a surrogate target centered on a point located along the laser entrance hole axis at a position 1356  $\mu\text{m}$  from target chamber center. The beams will then be moved from those positions by an amount calculated separately for each beam.

The pointing will be checked on a set of pointing experiments. The targets for these will be about 4000  $\mu\text{m}$  (5/32 inch) plastic spheres with a thin gold coating (supplied by Omega). Low-energy shots will be performed and the x-ray emission from the lasers will be imaged using time-integrated pinhole cameras. The position of the spots will then be compared to the predicted positions, and any necessary corrections to be pointing will then be determined.

### ***Target alignment***

Targets will be aligned by rotating the target so that the alignment fiber on the stalk is pointed toward the y-axis target viewer and then centering the sphere in the x- and y- target viewers. Rotation adjustment will be specified as the rotation needed to bring the target into alignment; i.e. align the fiber and then rotate x degrees clockwise as viewed from above. Any necessary adjustments to centering due to rotation should then be made.

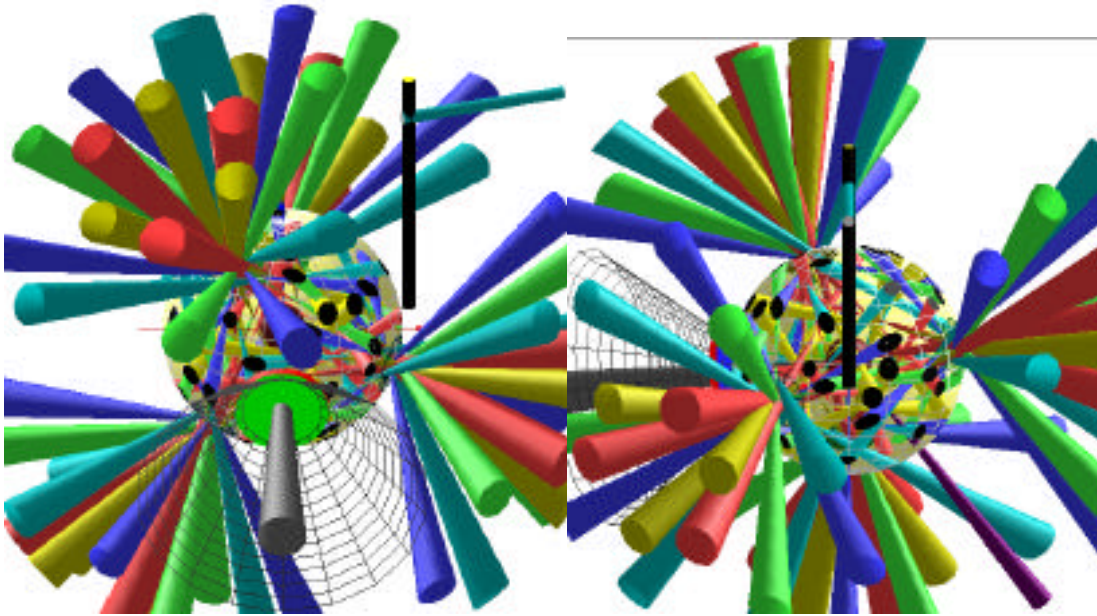


Figure 6: Target as seen in the X TVS (left) and Y TVS (right) when properly aligned. The open grid shows the location of the SOP shield for targets that have one and shows that the shield does not interfere with alignment. The SOP shield will not be used on this series of shots.

### **Experiments to be performed**

The experiments to be performed fall into two different categories: double shell high convergence implosions, and single shell high-convergence implosions. In addition, pointing sphere targets will be used on the first day to verify beam pointing prior to the start of experiments, and DANTE measurements will be made on the first day to verify the radiation temperature in empty hohlraums, for both pulse shapes.

#### ***Pointing sphere targets***

The pointing targets will consist of 5/32" diameter plastic sphere targets with a  $\sim 1 \mu\text{m}$  Au coating. The targets will be mounted similarly to hohlraums, i.e. with a stalk connected to the equator of the sphere and an alignment fiber to set the rotation (Fig. 6).

These targets will be provided by LLE.

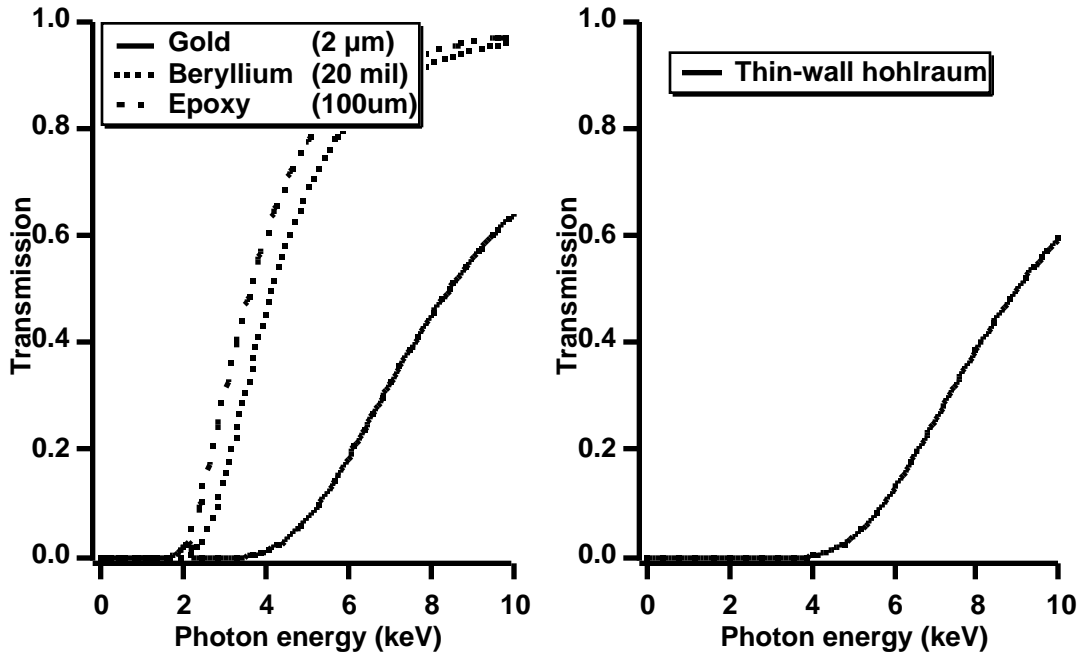


Figure 7: X-ray transmission of the components of a thin-wall hohlraum and the 20 mil beryllium filter typically used in gated x-ray imagers (left) and the total transmission function (right). The transmission is dominated by the 2- $\mu\text{m}$  gold layer of the hohlraum wall. The single shell implosions will use this imaging setup, while the double shell implosions will reduce the Be to 10 mil to enhance the net x-ray flux to the camera to compensate, in the imploded core imaging targets discussed below, for the somewhat higher initial  $rR$ .

### **Double shell implosion targets**

“Double-shell” targets will be tested during this series. These targets have previously been used on Nova and Omega experiments but have shown the same degradation in performance at their inherently high CR ( $>30$ ) as seen in single-shell implosions at high CR. In this experiment, an investigation of one possible source of the degradation, M band radiation asymmetries from the Au wall, will be investigated.

Nine targets will be used in this experiment, three with DD fill and six with DT fill. The primary diagnostics will be neutron-based. DD experiments will rely on Medusa to provide secondary neutron yield for determining  $R$  of the imploded fuel. DT will be used to allow high-accuracy neutron yield and burn history measurements. The anticipated yields, at less than 10% of the clean 1-D calculated yield, will be very low for the DD shots. Based on the previous Omega double shell implosions, in the absence of significant improvements in performance caused by the different materials and techniques, the DD

shots can be expected to push the envelope on neutron diagnostic capabilities. The DT shots will give easily measurable yields, bangtimes, and burn histories, even in the absence of anticipated improvements to the previous behavior due to target details. All available neutron diagnostics are to be run on all shots, including the pointing and drive measurement shots, in order to maximize the probability of data recovery, and to get good baseline data on noise levels in the absence of neutron production. Details of the diagnostic setup are in the attachment for the double shell targets.

Three target designs will be used:

1. A “standard” double shell design (23 mm wall GMB, 70 mm thick 30 mg/cc polystyrene foam interspace, and 76 mm thick outer CH ablator, filled with 36 atm DT). This design will be used to investigate the source of x-ray image artifacts seen in the previous series and to investigate the results of better assembly techniques. It provides the connection to past implosions.
2. A doped ablator variant of the “standard” design in which Br doped CH (C<sub>8</sub>H<sub>8.06</sub>Br<sub>0.194</sub>, 12.93% Br by weight) replaces the outer ablator. This design will inhibit the Au M band from reaching the inner, intermediate Z GMB, thus changing it’s response to M band asymmetries if present.
3. An imaging double shell design with the inner capsule consisting of a thin wall GMB (4 mm nominal) overcoated with 19 mm of CH in place of the normal 23 mm thick bare GMB in the “standard” target. The balance of the target is identical to the “standard” package. The main purpose of this target is to allow imaging of the imploded core, but in addition it has much different response to any M band incident on the inner capsule than does the “standard” double design.

Assuming 10% yield compared to clean calculations, the yield from the targets are expected to be  $2.9 \times 10^9$ ,  $6.6 \times 10^8$ , and  $5.4 \times 10^6$ , respectively.

### ***High-convergence single-shell implosion targets***

The optimized single-shell implosion capsules to be used here, are 440  $\mu\text{m}$  in inside diameter with a 30  $\mu\text{m}$  thick Ge-doped (1.1 % by atom) plastic wall. They will contain 50, 10, 7, and 4 atm DD; half of which will contain 0.1 atm Ar to enhance x-ray images of the imploded core. Neutronics form the primary means of diagnosis for the single-shell capsules. The entire neutron suite must be run on all shots to maximize the probability of data recovery. The neutron diagnostics and X-ray imaging of the imploded core and laser spots will be performed as spelled out in the accompanying attachments.

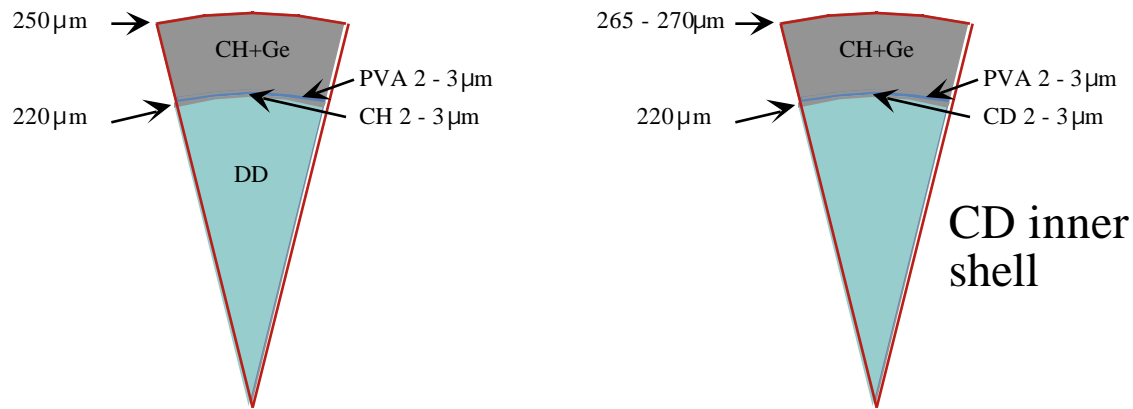


Figure 8: Left, the basic single-shell high-convergence target; DD filled, with or without 0.1 atm Ar dopant. Right, the HH filled (no Ar) CD shell capsule, designed to investigate mix of the fuel/pusher interface.

For the non-Ar doped single-shell capsules, the clean 1D LASNEX primary yields are  $1.9 - 3.1 \times 10^9$ ; whereas  $0.6 - 1.4 \times 10^9$  is expected for the doped capsules (both accurate to a factor of two or so). Therefore with, say, 50 - 10 % yield over 1D clean (YOC) for all shots, the DD range would be  $0.6 - 9.3 \times 10^8$ ; well within the optimum range of Medusa (calculating DT yield using table below). The anticipated CD-shell DD yields are  $1.4 - 3 \times 10^5$  (medusa DD range).

### **Metrology of high-convergence single-shell targets**

The DD filled capsules must be kept in dry ice prior to an experiment. (This requirement is not common to the double shell targets which use glass microballoons with fairly long confinement times.) The diffusion rate loss of deuterium, at room temperature, is believed to follow an exponential half life model with  $\tau = 24 - 36$  hours (approximately independent of fill pressures). Because of the uncertainty in  $\tau$ , the targets must be metrologized extremely quickly (a precisely known  $\tau$  would allow the DD loss to be calculated exactly); e.g. within an hour or less. During this time, the most important check will be the capsule location within the spherical hohlraum. Movement of the capsule during travel to Rochester is a possibility, since the formvar web is rather delicate. Thus, the capsule location will be metrologized and compared with pre-travel measurements. Secondly, the rotational alignment fiducial position will be checked and compared with the pre-travel figures. The position of the LEH's with respect to each other and the vertices of a tetrahedron will not of course change; these measurements will be obtained prior to boosting the capsules with DD.

### **References**

- [1] C. Decker, R. E. Turner, O. L. Landen, L. J. Suter, P. Amendt, H. N. Kornblum, B. A. Hammel, T. J. Murphy, J. Wallace, N. D. Delamater, P. Gobby, A. A. Hauer, G. R. Magelssen, J. A. Oertel, J. Knauer, F. J. Marshall, D.

Bradley, W. Seka, and J. M. Soures, Hohlraum radiation drive measurements on the Omega laser, *Phys. Rev. Lett.* **79**, 1491 (1997).

[2] T. J. Murphy, J. M. Wallace, N. D. Delamater, Cris W. Barnes, P. Gobby, A. A. Hauer, E. Lindman, G. Magelssen, J. B. Moore, J. A. Oertel, R. Watt, O. L. Landen, P. Amendt, M. Cable, C. Decker, B. A. Hammel, J. Koch, L. J. Suter, R. E. Turner, R. J. Wallace, F. J. Marshall, D. Bradley, R. S. Craxton, R. Keck, J. P. Knauer, R. Kremens, and J. D. Schnittman, Hohlraum symmetry experiments with multiple beam cones on the Omega Laser Facility, *Phys. Rev. Lett.* **81**, 108 (1998).

[3] T. J. Murphy, J. M. Wallace, N. D. Delamater, Cris W. Barnes, P. Gobby, A. A. Hauer, E. L. Lindman, G. Magelssen, J. B. Moore, J. A. Oertel, R. Watt, O. L. Landen, P. Amendt, M. Cable, C. Decker, B. A. Hammel, J. Koch, L. J. Suter, R. E. Turner, R. J. Wallace, F. J. Marshall, D. Bradley, R. S. Craxton, R. Keck, J. P. Knauer, R. Kremens, and J. D. Schnittman, Indirect drive experiments utilizing multiple beam cones in cylindrical hohlraums on OMEGA, *Phys. Plasmas* **5**, 1960 (1998).

[4] T. J. Murphy, J. Wallace, K. A. Klare, J. A. Oertel, C. W. Barnes, N. D. Delamater, P. Gobby, A. A. Hauer, E. Lindman, G. Magelssen, O. L. Landen, P. Amendt, C. Decker, L. Suter, B. Hammel, R. Turner, R. Wallace, R. S. Craxton, F. J. Marshall, D. Bradley, D. Harding, K. Kearney, R. Keck, J. Knauer, R. Kremens, W. Seka, M. Cable, and J. Schnittman, Experiments utilizing spherical hohlraums with tetrahedral illumination on Omega, *Bull. Am. Phys. Soc.* **42**, 2008 (1997).

[5] J. M. Wallace *et al.*, Measurements of radiative drive symmetry in tetrahedral hohlraums, to be published.

[6] J. D. Schnittman, R. S. Craxton, Indirect-drive radiation uniformity in tetrahedral hohlraums, *Phys. Plasmas* **3**, 3786 (1996).

[7] D. W. Phillion, S. M. Pollaine, Dynamical compensation of irradiation nonuniformities in a spherical hohlraum illuminated with tetrahedral symmetry, *Phys. Plasmas* **1**, 2963 (1995).

[8] T. J. Murphy, Tetrahedral Hohlraum Proof-of-Principle Experiments on Omega ID2, March 24-28, 1997 (unpublished).

[9] K. A. Klare, J. M. Wallace, and D. Drake, Tetrahedral hohlraum visualization and pointings, *Bull. Am. Phys. Soc.* **42**, 1993 (1997).

[10] J. A. Oertel, T. J. Murphy, R. R. Berggren, R. F. Horton, J. Faulkner, R. Schmell, D. Little, T. Archuleta, J. Lopez, and J. Velarde, A multipurpose TIM-based telescope for Omega and the Trident laser Facilities, submitted to *Rev. Sci. Instrum.*



[11] Douglas C. Wilson, Paul A. Bradley, Nelson M. Hoffman, Fritz J. Swenson, David P. Smitherman, Robert E. Chrien, Robert W. Margevicius, D. J. Thoma, Larry R. Foreman, James K. Hoffer, S. Robert Goldman, and Stephen E. Caldwell, Thomas R. Dittrich, Steven W. Haan, Michael M. Marinak, Stephen M. Pollaine, and Jorge J. Sanchez, The development and advantages of beryllium capsules for the National Ignition Facility, Phys. Plasmas 5, 1953 (1998).

## **Attachments**

- (1) Detailed day-by-day shot plan
- (2) Diagnostic setup report for double-shell implosions
- (3) Notes on x-ray and neutron diagnostics for single-shell implosions
- (4) Complete setup for all shots
- (5) Pointing coordinates (identical to pages 9 - 10)
- (6) Hohlräum design and LEH locations in Omega's coordinates
- (7) Views of hohlräum (with 550 micron single-shell capsule, and without 100 micron epoxy coating outer hohlräum) from all six TIMs, plus TV-X and TV-Y views. 43x hohlräum-mounted pinhole arrays are shown, so are the laser spots
- (8) LLE site map
- (9) Distribution

Day 1 (03/02/99) 1 nsec square	Day 2 (03/03/99) PS26 shaped	Day 3 (03/04/99) PS26 shaped
pointing shot #1 RID #	50 atm D2, 0.1 atm Ar LLNL design RID # 5447	7 atm D2, 0.1 atm Ar, LANL design RID # 5461
pointing shot #2 (shot may be dropped) RID #	50 atm D2, 0.1 atm Ar LLNL design RID # 5448	4 atm D2, 0.1 atm Ar, LANL design RID # 5462
drive shot 1 nsec square #1 RID #	50 atm D2, 0.1 atm Ar LLNL design RID # 5449	4 atm D2, 0.1 atm Ar, LANL design RID # 5463
double shell #1 RID #	10 atm D2, 0.1 atm Ar LLNL design RID # 5450	4 atm D2, 0.1 atm Ar, LANL design RID # 5464
double shell #2 RID #	10 atm D2, 0.1 atm Ar LLNL design RID # 5451	50 atm D2 LLNL design RID # 5465
double shell #3 RID #	10 atm D2, 0.1 atm Ar LLNL design RID # 5452	50 atm D2 LLNL design RID # 5466
double shell #4 RID #	7 atm D2, LANL design RID # 5453	50 atm D2 LLNL design RID # 5467
double shell #5 RID #	7 atm D2, LANL design RID # 5454	10 atm D2 LLNL design RID # 5468
double shell #6 RID #	7 atm D2, LANL design RID # 5455	10 atm D2 LLNL design RID # 5469
double shell #7 RID #	4 atm D2, LANL design RID # 5456	10 atm D2 LLNL design RID # 5470
double shell #8 RID #	4 atm D2, LANL design RID # 5457	50 atm H2 CD shell RID # 5471
double shell #9 RID #	4 atm D2, LANL design RID # 5458	50 atm H2 CD shell RID # 5472
drive shot PS26 shaped #1 RID # 5445	7 atm D2, 0.1 atm Ar, LANL design RID # 5459	20 atm H2 CD shell RID # 5473
drive shot PS26 shaped #2 RID # 5446	7 atm D2, 0.1 atm Ar, LANL design RID # 5460	20 atm H2 CD shell RID # 5474



## (Attachment 2.)

### Double shell diagnostics on the March 1, 1999 Double Shell implosions.

This assumes the hohlraum is aligned along the H7 axis as in all the shots the week of March 1.

Scale 1.2 tetrahedral hohlraums, 28 kJ, 1 ns flattop, no DPP, no SSD.

- A) Standard double shell: 23 mm GMB, normal 30 mg/cc foam, normal CH ablator. 36 Atm DT. Calculated clean Y  $2.9 \times 10^{10}$  DT neutrons. 1.3 keV  $T_{ion}$ , 0.015 gm. $cm^2$  rDR, CR=38. Improved assembly technique and metrology.
- B) Doped ablator targets: Br doped ablator (sample measurements: C8H8.06Br0.194, 1.1936% by atomic fraction, 12.93% by weight, density 1.145 g/cc), normal 30 mg/cc foam interspace, normal 23 mm GMB. 36 Atm DT. Calculated clean Y  $6.6 \times 10^9$  DT neutrons, 1.0 keV  $T_{ion}$ , 0.011 gm/ $cm^2$  rDR, CR=32. (Note: we aimed at C8H7.85Br0.15, 0.9375% by atomic fraction, 10.93% by weight but missed a bit on the high side.)
- C) Thin wall GMB core imaging shots: 4 mm GMB + 19 mm CH overcoat, normal 30 mg/cc foam interspace, normal CH ablator. 36 Atm DD. Calculated clean Y  $5.4 \times 10^7$  DD neutrons, 0.83 keV  $T_{ion}$ , 0.0062 gm/ $cm^2$  rDR, CR = 23.

### Neutron diagnostics for March 1999

Neutron diagnostic	Shot type	Calc. Y	Ant. Y	Ant. YOC	comments
Cu activation	DT (A,B)	$.66-3 \times 10^{10}$	$.66-3 \times 10^8$	1%	marginal
Scintillator	DT (A,B)	$.66-3 \times 10^{10}$	$.66-3 \times 10^8$	1%	
Scintillator	DD ( C )	$5.4 \times 10^7$	$5.4 \times 10^5$	1%	lower end of range
Medusa	DT (A,B)	$.66-3 \times 10^{10}$	$.66-3 \times 10^8$	1%	rR marginal
Medusa	DD ( C )	$5.4 \times 10^7$	$5.4 \times 10^5$	1%	$T_{ion}$ marginal
Omega BT	All	$0.0054-3 \times 10^{10}$	$0.0054-3 \times 10^8$	1%	
LANL BT	All	$0.0054-3 \times 10^{10}$	$0.0054-3 \times 10^8$	1%	developmental
NTD	DT (A,B)	$.66-3 \times 10^{10}$	$.66-3 \times 10^8$	1%	

## Imaging diagnostics for March 1999

Imaging Camera	Shot type	TIM	Axis	Timing	Mag	Pinhole ( _ m)	Filtration	Gain setting	Function
QXI (LANL)	DD ( C )	2	LEH	To+2.0ns 250 ps dt	12x	5 GXI style	10 mil Be CsI PC	+50 volt	imploded core image
QXI (LANL)	DT (A,B)	2	LEH	To+0.25ns 250 ps dt	8x	5 GXI style	10 mil Be CsI PC	+50 volt	early time Au wall backlit capsule image
GXI-T (LANL)	All	3		To (1ns window)	2x	10	Au PC 10 mil Be	-100 volt (?)	gated spot images
Pinhole camera	All		All	static	4x	std	6 mil Be only		static spots + core
XRSC	none								
GMXI	none								
SOP	none								

### Other diagnostics required.

Backscatter fraction in 1 or more incident beams.

Beam 25 calorimetry BS will be run by Omega ops.

Beam 30 BS station will be run by LANL experimental team

Incident energy and pulse shape.

Preshot target image as seen from TIM 2 LEH (from MST).

**(Attachment 3.)**

**High-convergence single-shell implosion targets diagnostic setup**

The optimized single-shell implosion capsules to be used here, are 440  $\mu\text{m}$  in inside diameter with a 30  $\mu\text{m}$  thick Ge-doped (1.1 % by atom) plastic wall. They will contain 50, 10, 7, and 4 atm  $\text{D}_2$ ; half of which will contain 0.1 atm Ar to enhance x-ray images of the imploded core.

Expected ion temperatures for each DD fill pressure, with and without Ar dopant, are shown in the below table.

<b>DD pressure</b>	<b>Ion temp (keV) with Ar</b>	<b>Ion temp (keV) no Ar</b>
50 atm	1.1	1.2
10 atm	1.6	1.8
7 atm	1.6	1.9
4 atm	1.7	2.0

<b>DD pressure</b>	<b>DT/DD with Ar</b>	<b>DT/DD no Ar</b>
50 atm	0.0018	0.0015
10 atm	0.0015	0.0011
7 atm	0.0015	0.0011
4 atm	0.0010	0.0011

The ratio of DT to DD (secondary to primary) neutrons is shown above. For the non-Ar doped single-shell capsules, the clean 1D LASNEX primary yields are  $1.9 - 3.1 \times 10^9$ ; whereas  $0.6 - 1.4 \times 10^9$  is expected for the doped capsules (both accurate to a factor of two or so). Therefore with, say, 50 - 10 % yield over 1D clean (YOC) for all shots, the DD range would be  $0.6 - 9.3 \times 10^8$ ; well within the optimum range of Medusa (calculating DT yield using above table). The anticipated CD-shell DD yields are  $1.4 - 3 \times 10^5$  (medusa DD range).

Neutronics form the primary means of diagnosis for both the double- and single-shell capsules. However, both capsule designs require somewhat different instruments. The primary diagnostics for the single-shells are shown in the below table.

instrument	purpose	point of contact
medusa	secondary yield and spectra	V. Yu. Glebov/C. Stoekl
scintillator counters	primary yield	V. Yu. Glebov/C. Stoekl
3.0 meter NTOF	ion temperature	V. Yu. Glebov/C. Stoekl
LLE bangtime		V. Yu. Glebov/C. Stoekl
LANL bangtime		J. L. Jimmerson (LANL)

Various x-ray imaging instruments form the secondary diagnostics for the single-shell capsule. Of most importance are QXI in TIM2 and KB3 in H13F, since they view the capsule through LEH's. KB3, located in H13F, looks directly into an LEH. This instrument has four grazing incidence channels plus one pin hole image (10  $\mu\text{m}$  diameter pinhole and 22.6x magnification). Generally, only time-integration onto film is possible. However, for this experiment we may have an x-ray CCD (Fred Marshall) over one channel. KB images are 20.3x, and all five channels are usually dispersed by a grating. For our experiment, however, this will be removed. Channels 1 & 2 are filtered by 6 mil of Be (the minimum), whereas 3 & 4 have 4 mils of polypropylene as additional filtering. One can adjust the spectral filtering by using 0.5 mil increments of Al. The 0.7 degree mirrors are iridium coated, and the estimated spatial resolution is of order 3 - 10  $\mu\text{m}$  (allowing for motional blur of typical directly-driven imploding capsules, time-integrated onto film). KB1 located in H8 is directly opposite KB3, and therefore looks through an LEH antipode. This device differs in the reduced magnification (13x for KB and pinhole images) and spatial resolution; plus the use of a 5 rather than 10  $\mu\text{m}$  pinhole. This instrument *will* have a diffraction grating.

Omega has four x-ray framing cameras (XRFC's), each capable of capturing 16 frames (four frames per strip, with adjustable interstrip timing). Apparently LANL QXI is the most sensitive camera, and so this instrument will be located in TIM2 for an LEH view. 12x magnification (the maximum available) and 5  $\mu\text{m}$  pinholes (provided by Los Alamos, and metrologized by Guy Bennett) will be employed for optimum image quality of the imploding core. The below table lists the x-ray imaging diagnostics.

<b>instrument</b>	<b>location</b>	<b>purpose</b>	<b>priority</b>
KB#3 (no grating)	H13F (LEH view)	20.3x 4-channel, implosion	1
LANL QXI	TIM2 (LEH view)	12x or 43x implosion	1
LANL GXI-T	TIM3	2x laser spots	1
XRFC2	TIM4	12x implosion	3
XRFC1	TIM5	2x laser spots	3
XRFC3/SXRFC	TIM6	3x monitor LEH closure	1 or 2
PH1	P12A	4x	2
PH2	H9C	4x	2
PH3	H8C	4x	2
PH4	H3C	4x	2
PH5	H13C (LEH view)	4x	2
PH6	H12C	4x	2
GMXI/KB#2	H9F	13x tuned to Ar H-beta	2
KB#1	H8F	13x implosion	2

***Special issues for x-ray diagnostics during single-shell shots***

- There are two LEH views: TIM2 and H13. KB3 microscope, located in H13F, will have its grating removed. Use no filtering on channels 1 & 2, but use 4 mil polypropylene across 3 & 4. Leave pinhole unfiltered.
- QXI in TIM2 with 20 mil Be filter and 5 micron Los Alamos pinholes (metrologized by Guy Bennett), or 43x hohlraum-mounted pinhole arrays. Set for 12x magnification (essential to use correct 12x alignment pointer). Replace pinholes after each shot, but do not upset nose cone position. Film must always make precise contact with MCP. TIM2 alignment must never change from one shot to another. Set timing as  $T_0 + 1.9$  nsec and 250 psec interstrip timing. Gain = + 50 V.
- SXRFC (i.e. XRFC3 with LLNL nose cone, located in TIM6) and dante will be used.



Diagnostic setup sheet

Campaign: ID6-FY99 Tetrahedral Hohltraums

Day: #1 Pulse shape: 1 nsec square  
 Shots: 1 & 2 Energy/beam (UVOT): 100 J  
 PI: Delamater Beams on Target: 60  
 Total Energy on Target: 6 kJ

Target: 4 mm pointing sphere  
 Alignment: Centered with fidu pointing at Y TVS

Purpose: check pointing and time instruments

TIM-based diagnostics

TIM	location	Instrument	Pri.	Magnification	Pinholes	Filtering	Timing	Strip Timing	Bias	Notes
1	P3	TIM-based PHC	1	4	10 μm	5 mil Be				Pointing verification
2	H7	QXI	2	2	10 μm	10 mil Be	To + 0 nsec	250 psec	+50 V	Timing, alignment and exposure
3	H18	GXI-T	2	2	10 μm	10 mil Be	To + 0 nsec	250 psec	-100 V	Timing, alignment and exposure
4	P6	TIM-based PHC	1	4	10 μm	5 mil Be				Pointing verification
5	H14	TIM-based PHC	1	4	10 μm	5 mil Be				Pointing verification
6	P7	XRFC3/SXRFC snout	2	3	25/10/25	special	To + 0.1 nsec	250 psec		Timing, alignment and exposure

Fixed x-ray diagnostics

			Pri.	Magnification	Pinholes	Filtering	Timing	Strip Timing	Bias	Notes
KBs	H8F	KB1	not used							
	H9F	KB2/GMXI	not used							
	H13F	KB3	not used							
PHCs	P12A	XRPC #1	1	4	10 μm	std Be only				Pointing verification
	H9C	XRPC #2	1	4	10 μm	std Be only				Pointing verification
	H8C	XRPC #3	1	4	10 μm	std Be only				Pointing verification
	H3C	XRPC #4	1	4	10 μm	std Be only				Pointing verification
	H13C	XRPC #5	1	4	10 μm	std Be only				Pointing verification
	H12C	XRPC #6	1	4	10 μm	std Be only				Pointing verification
Dante	H16I	Dante	2							Time Dante
IXRSC	H3F	Imaging x-ray streak	2							Observes alignment problems

Neutron Diagnostics

		Pri.	Type	Expected Yield	Bang time	Notes
H15D	LANL Bangtime	2	x rays	-	0.5 nsec	Neutron bang time for testing and timing
P2D	LLE Bangtime	2	x rays	-	0.5 nsec	Look for x-rays to confirm timing

Laser Diagnostics

Beam 25 backscatter	2					Calorimetry only, streaking not required
Beam 30 backscatter	2					Calorimetry only, streaking not required
P510A streaks	2	Clusters 4 & 5				
Pulseshape measurements	2	Beams 19 & 20				

Note

XRFC3/SXRFC should be pointed to monitor Dante Hole (LEH D), X=-808 μm, Y=-263 μm, Z=-1113 μm. All other diagnostics pointed to TCC

Diagnostic setup sheet

Campaign: ID6-FY99 Tetrahedral Hohltraums

Day: #1	Pulse shape: 1 nsec square
Shots: 3	Energy/beam (UVOT): 450 J
PI: Delamater	Beams on Target: 60
	Total Energy on Target: 27 kJ

Target: drive  
Alignment: Centered with fidu pointing at Y TVS

Purpose: 1 nsec drive shot

TIM-based diagnostics

TIM	location	Instrument	Pri.	Magnification	Pinholes	Filtering	Timing	Strip Timing	Bias	Notes
1	P3									
2	H7	QXI	2	8	5 μm	10 mil Be	To + 0 nsec	250 psec	+50 V	Timing, alignment, image integrity, and exposure
3	H18	GXI-T	2	2	10 μm	10 mil Be	To + 0 nsec	250 psec	-100 V	Timing, alignment, image integrity, and exposure
4	P6									
5	H14									
6	P7	XRFC3/SXRFC snout	1	3	25/10/25	special	To + 0.1 nsec	250 psec		PRIMARY DIAGNOSTIC

Fixed x-ray diagnostics			Pri.	Magnification	Pinholes	Filtering	Timing	Strip Timing	Bias	Notes
KBs	H8F	KB1	not used							
	H9F	KB2/GMXI	not used							
	H13F	KB3	not used							
PHCs	P12A	XRPC #1	2	4	10 μm	std Be only				
	H9C	XRPC #2	2	4	10 μm	std Be only				
	H8C	XRPC #3	2	4	10 μm	std Be only				
	H3C	XRPC #4	2	4	10 μm	std Be only				
	H13C	XRPC #5	2	4	10 μm	std Be only				
	H12C	XRPC #6	2	4	10 μm	std Be only				
Dante	H16I	Dante	1							PRIMARY DIAGNOSTIC
IXRSC	H3F	Imaging x-ray streak	2							Observes alignment problems

Neutron Diagnostics		Pri.	Type	Expected Yield	Bang time	Notes
H15D	LANL Bangtime	2	x rays	-	0.5 nsec	Neutron bang time for testing and timing
P2D	LLE Bangtime	2	x rays	-	0.5 nsec	Look for x-rays to confirm timing

Laser Diagnostics		Pri.	Notes
Beam 25 backscatter		1	Calorimetry only, streaking not required
Beam 30 backscatter		1	Calorimetry only, streaking not required
P510A streaks		1	Clusters 4 & 5
Pulseshape measurements		1	Beams 19 & 20

Note

XRFC3/SXRFC should be pointed to monitor Dante Hole (LEH D), X=-808 μm, Y=-263 μm, Z=-1113 μm. All other diagnostics pointed to TCC

Diagnostic setup sheet

Campaign: ID6-FY99 Tetrahedral Hohlräume

Day: #1	Pulse shape: 1 nsec square
Shots: 4 to 9	Energy/beam (UVOT): 450 J
Pl: Watt	Beams on Target: 60
	Total Energy on Target: 27 kJ

Target: DT double-shell  
 Alignment: Centered with fidu pointing at Y TVS

Purpose: double-shells

TIM-based diagnostics

TIM	location	Instrument	Pri.	Magnification	Pinholes	Filtering	Timing	Strip Timing	Bias	Notes
1	P3									
2	H7	QXI	1	12	5 µm	10 mil Be	To + 1.75 nsec	250 psec	+50 V	Backlit core
3	H18	GXI-T	1	2	10 µm	10 mil Be	To + 0 nsec	250 psec	-100 V	Laser spots
4	P6									
5	H14									
6	P7									

Fixed x-ray diagnostics

			Pri.	Magnification	Pinholes	Filtering	Timing	Strip Timing	Bias	Notes
KBs	H8F	KB1	not used							
	H9F	KB2/GMXI	not used							
	H13F	KB3	not used							
PHCs	P12A	XRPC #1	2	4	10 µm	std Be only				
	H9C	XRPC #2	2	4	10 µm	std Be only				
	H8C	XRPC #3	2	4	10 µm	std Be only				
	H3C	XRPC #4	2	4	10 µm	std Be only				
	H13C	XRPC #5	2	4	10 µm	std Be only				
	H12C	XRPC #6	2	4	10 µm	std Be only				
Dante	H16I	Dante	1							Continue Dante measurements
IXRSC	H3F	Imaging x-ray streak	2							NOT USED shots 4 to 9

Neutron Diagnostics

			Pri.	Type	Expected Yield	Bang Time	Notes
	P10	Medusa/nToF	1	DD	see Watt	see Watt	Secondary DT yield
	P12B	Neutron scintillator	1				Primary DD yield
	P9A	Indium activation	1				Primary DD yield
	P9C	Copper activation	1				Primary DT yield
	P12	3.0 meter nToF	1				Ion temperature
	P2D	LLE Bangtime	1				Neutron bang time
	H15D	LANL Bangtime	1				Neutron bang time
	H5I	nTD	1				Neutron burn history on DT shots

Laser Diagnostics

Beam 25 backscatter	1					Calorimetry only, streaking not required
Beam 30 backscatter	1					Calorimetry only, streaking not required
P510A streaks	1	Clusters 4 & 5				
Pulseshape measurements	1	Beams 19 & 20				

Note

XRFC3/SXRFC should be pointed to monitor Dante Hole (LEH D), X=-808 µm, Y=-263 µm, Z=-1113 µm. All other diagnostics pointed to TCC

Diagnostic setup sheet

Campaign: ID6-FY99 Tetrahedral Hohlräume

Day: #1 Pulse shape: 1 nsec square  
 Shots: 10 to 12 Energy/beam (UVOT): 450 J  
 Pl: Watt Beams on Target: 60  
 Total Energy on Target: 27 kJ

Target: DD double-shell  
 Alignment: Centered with fidu pointing at Y TVS

Purpose: double-shells

TIM-based diagnostics

TIM	location	Instrument	Pri.	Magnification	Pinholes	Filtering	Timing	Strip Timing	Bias	Notes
1	P3									
2	H7	QXI	1	8	5 µm	10 mil Be	To + 250 psec	250 psec	+50 V	Backlit core
3	H18	GXI-T	1	2	10 µm	10 mil Be	To + 0 nsec	250 psec	-100 V	Laser spots
4	P6									
5	H14									
6	P7	XRFC3/SXRFC snout	1	3	25/10/25	special	To + 0.1 nsec	250 psec		Continue to monitor LEH

Fixed x-ray diagnostics			Pri.	Magnification	Pinholes	Filtering	Timing	Strip Timing	Bias	Notes
KBs	H8F	KB1	not used							
	H9F	KB2/GMXI	not used							
	H13F	KB3	not used							
PHCs	P12A	XRPHC #1	2	4	10 µm	std Be only				
	H9C	XRPHC #2	2	4	10 µm	std Be only				
	H8C	XRPHC #3	2	4	10 µm	std Be only				
	H3C	XRPHC #4	2	4	10 µm	std Be only				
	H13C	XRPHC #5	2	4	10 µm	std Be only				
	H12C	XRPHC #6	2	4	10 µm	std Be only				
Dante	H16I	Dante	1							Continue Dante measurements
IXRSC	H3F	Imaging x-ray streak	2							Observes alignment problems

Neutron Diagnostics			Pri.	Type	Expected Yield	Bang Time	Notes
P10	Medusa/nToF		1	DT	see Watt	see Watt	Secondary DT yield
P12B	Neutron scintillator		1				Primary DD yield
P9A	Indium activation		1				Primary DD yield
P9C	Copper activation		1				Primary DT yield
P12	3.0 meter nToF		1				Ion temperature
P2D	LLE Bangtime		1				Neutron bang time
H15D	LANL Bangtime		1				Neutron bang time
H5I	nTD		1				Neutron burn history on DT shots

Laser Diagnostics			Pri.	Notes
Beam 25 backscatter			1	Calorimetry only, streaking not required
Beam 30 backscatter			1	Calorimetry only, streaking not required
P510A streaks		Clusters 4 & 5	1	
Pulseshape measurements		Beams 19 & 20	1	

Note XRFC3/SXRFC should be pointed to monitor Dante Hole (LEH D), X=-808 µm, Y=-263 µm, Z=-1113 µm. All other diagnostics pointed to TCC

Diagnostic setup sheet

Campaign: ID6-FY99 Tetrahedral Hohlräume

Day: #1	Pulse shape: PS26
Shots: 13 to 14	Energy/beam (UVOT): 340 J
PI: Bennett	Beams on Target: 60
	Total Energy on Target: 20.4 kJ

Target: drive  
Alignment: Centered with fidu pointing at Y TVS

Purpose: PS26 drive shot

TIM-based diagnostics

TIM	location	Instrument	Pri.	Magnification	Pinholes	Filtering	Timing	Strip Timing	Bias	Notes
1		P3								
2	H7	QXI	3	8	5 µm	20 mil Be	To + 2.1 nsec	250 psec	+50 V	Hohlraum background radiation should be zero; filter check
3	H18	GXI-T	1	2	10 µm	10 mil Be	To + 0.25 nsec	250 psec	-100 V	Laser spots
4	P6	XRFC2	3	12	5 µm	10 mil Be	To + 2.1 nsec	250 psec	+50 V	Hohlraum background radiation should be zero; filter check
5	H14	XRFC1	1	2	10 µm	20 mil Be	To + 0.25 nsec	500 psec	+200 V	Laser spots
6	P7	XRFC3/SXRFC snout	1	3	25/10/25	special	To + 0.25 nsec	500 psec	+300 V	PRIMARY DIAGNOSTIC

Fixed x-ray diagnostics			Pri.	Magnification	Pinholes	Filtering	Timing	Strip Timing	Bias	Notes
KBs	H8F	KB1	not used							
	H9F	KB2/GMXI	3	13		To(a) +1.9 ns, To(b) + 2.6 ns		max gain	Tune to Ar H-beta (3.935 keV); may retune to 5 keV or higher	
	H13F	KB3	not used							
PHCs	P12A	XRPC #1	2	4	10 µm	std Be only				
	H9C	XRPC #2	2	4	10 µm	std Be only				
	H8C	XRPC #3	2	4	10 µm	std Be only				
	H3C	XRPC #4	2	4	10 µm	std Be only				
	H13C	XRPC #5	2	4	10 µm	std Be only				
	H12C	XRPC #6	2	4	10 µm	std Be only				
Dante	H16I	Dante	1						PRIMARY DIAGNOSTIC. Assume ~ 190 eV peak	
IXRSC	H3F	Imaging x-ray streak	2						Observes alignment problems	

Neutron Diagnostics		Pri.	Type	Expected Yield	Bang time	Notes
H15D	LANL Bangtime	2	x rays	-	1.3 nsec	Neutron bang time for testing and timing
P2D	LLE Bangtime	2	x rays	-	1.3 nsec	Look for x-rays to confirm timing

Laser Diagnostics		Pri.	Notes
Beam 25 backscatter		1	Calorimetry only, streaking not required
Beam 30 backscatter		1	Calorimetry only, streaking not required
P510A streaks	Clusters 4 & 5	1	
Pulseshape measurements	Beams 19 & 20	1	

Note

XRFC3/SXRFC should be pointed to monitor Dante Hole (LEH D), X=-808 µm, Y=-263 µm, Z=-1113 µm. All other diagnostics pointed to TCC  
See Jon Wallace about fine tuning PS26

Diagnostic setup sheet

Campaign: ID6-FY99 Tetrahedral Hohlräume

Day:	2 & 3	Pulse shape:	PS26	
Shots:	15 to 38	Energy/beam (UVOT):	340	J
PI:	Bennett	Beams on Target:	60	
		Total Energy on Target:	20.4	kJ

Target: DD single-shell  
 Alignment: Centered with fidu pointing at Y TVS

Purpose: achieve high-convergence in a tetrahedral hohlraum

TIM-based diagnostics

TIM	location	Instrument	Pri.	Magnification	Pinholes	Filtering	Timing	Strip Timing	Bias	Notes
1		P3								
2	H7	QXI	1	12 or 43	5 $\mu$ m	20 mil Be	To + 1.9 nsec	250 psec	+50 V	View implosion through LEH B
3	H18	GXI-T	2	2	10 $\mu$ m	10 mil Be	To + 0.25 nsec	250 psec	-100 V	Laser spots
4	P6	XRFC2	3	12	5 $\mu$ m	10 mil Be	To + 1.9 nsec	250 psec	+50 V	Looks at implosion through wall, and ~ orthogonal to TIM2 camera
5	H14	XRFC1	3	2	10 $\mu$ m	20 mil Be	To + 0.25 nsec	500 psec	+200 V	Monitor laser spots through hohlraum antipode
6	P7	XRFC3/SXRFC snout	1	3	25/10/25	special	To + 0.25 nsec	500 psec	+300 V	Continue to monitor LEH

Fixed x-ray diagnostics

			Pri.	Magnification	Pinholes	Filtering	Timing		Notes
KBs	H8F	KB1	2	13		no additional			With grating
	H9F	KB2/GMXI	3	13			To(a) + 1.9 ns, To(b) + 2.6 ns	max gain	Tune to Ar H-beta (3.935 keV); may retune to 5 keV or higher
	H13F	KB3	1	20.3	none on a & b, 4 mil poly on c & d				View implosion through LEH C, grating removed, x-ray CCD over c or d
PHCs	P12A	XRPHC #1	2	4	10 $\mu$ m	std Be only			
	H9C	XRPHC #2	2	4	10 $\mu$ m	std Be only			
	H8C	XRPHC #3	2	4	10 $\mu$ m	std Be only			
	H3C	XRPHC #4	2	4	10 $\mu$ m	std Be only			
	H13C	XRPHC #5	2	4	10 $\mu$ m	std Be + 0.5 mil Al			View implosion through LEH C
	H12C	XRPHC #6	2	4	10 $\mu$ m	std Be only			
Dante	H16I	Dante	1						Continue Dante measurements. Assume ~ 190 eV peak
IXRSC	H3F	Imaging x-ray streak	3						Observes alignment problems

Neutron Diagnostics

			Pri.	Type	Expected Yield	Bang time	Notes
P10	Medusa/nToF		1	DD	0.6 - 9.3 x 10 <sup>8</sup>	~ 2.4 nsec	Secondary (DT) yield and energy spectra
P12B	Neutron scintillator		1				Primary (DD) yield
P12	3.0 meter nToF		1				Ion temperature
P2D	LLE Bangtime		1				Neutron bang time, plan for ~ 2.4 nsec
H15D	LANL Bangtime		1				Neutron bang time, plan for ~ 2.4 nsec

Laser Diagnostics

Beam 25 backscatter	1					Calorimetry only, streaking not required
Beam 30 backscatter	1					Calorimetry only, streaking not required
P510A streaks	1	Clusters 4 & 5				
Pulseshape measurements	1	Beams 19 & 20				

Note

XRFC3/SXRFC should be pointed to monitor Dante Hole (LEH D), X=-808  $\mu$ m, Y=-263  $\mu$ m, Z=-1113  $\mu$ m. All other diagnostics pointed to TCC  
 See Jon Wallace about fine tuning PS26

Diagnostic setup sheet

Campaign: ID6-FY99 Tetrahedral Hohlräume

Day: #3 Pulse shape: PS26  
 Shots: 39 to 42 Energy/beam (UVOT): 340 J  
 PI: Bennett Beams on Target: 60  
 Total Energy on Target: 20.4 kJ

Target: CD-shell  
 Alignment: Centered with fidu pointing at Y TVS

Purpose: study "mix" in a tetrahedral hohlraum

TIM-based diagnostics

TIM	location	Instrument	Pri.	Magnification	Pinholes	Filtering	Timing	Strip Timing	Bias	Notes
1		P3								
2	H7	QXI	1	12 or 43	5 µm	20 mil Be	To + 2.7 nsec	250 psec	+50 V	View implosion through LEH B
3	H18	GXI-T	2	2	10 µm	10 mil Be	To + 0.25 nsec	250 psec	-100 V	Laser spots
4	P6	XRFC2	3	12	5 µm	10 mil Be	To + 2.7 nsec	250 psec	+50 V	Looks at implosion through wall, and ~ orthogonal to TIM2 camera
5	H14	XRFC1	3	2	10 µm	20 mil Be	To + 0.25 nsec	500 psec	+200 V	Monitor laser spots through hohlraum antipode
6	P7	XRFC3/SXRFC snout	1	3	25/10/25	special	To + 0.25 nsec	500 psec	+300 V	Continue to monitor LEH

Fixed x-ray diagnostics

			Pri.	Magnification	Pinholes	Filtering	Timing		Notes
KBs	H8F	KB1	2	13		no additional			with grating
	H9F	KB2/GMXI	3	13			To(a) + 1.9 ns, To(b) + 2.6 ns	max gain	
	H13F	KB3	1	20.3	none on a & b, 4 mil poly on c & d				View implosion through LEH C, grating removed, x-ray CCD over c or d
PHCs	P12A	XRPC #1	2	4	10 µm	std Be only			
	H9C	XRPC #2	2	4	10 µm	std Be only			
	H8C	XRPC #3	2	4	10 µm	std Be only			
	H3C	XRPC #4	2	4	10 µm	std Be only			
	H13C	XRPC #5	2	4	10 µm	std Be + 0.5 mil Al			View implosion through LEH C
	H12C	XRPC #6	2	4	10 µm	std Be only			
Dante	H16I	Dante	1						Continue Dante measurements. Assume ~ 190 eV peak
IXRSC	H3F	Imaging x-ray streak	3						Observes alignment problems

Neutron Diagnostics

			Pri.	Type	Expected Yield	Bang time	Notes
P10	Medusa/nToF		1	DD	1.4 - 3 x 10 <sup>4</sup>	~ 3.2 nsec	Secondary (DT) yield and energy spectra
P12B	Neutron scintillator		1				Primary (DD) yield
P12	3.0 meter nToF		1				Ion temperature
P2D	LLE Bangtime		1				Neutron bang time, plan for ~ 3.2 nsec
H15D	LANL Bangtime		1				Neutron bang time, plan for ~ 3.2 nsec

Laser Diagnostics

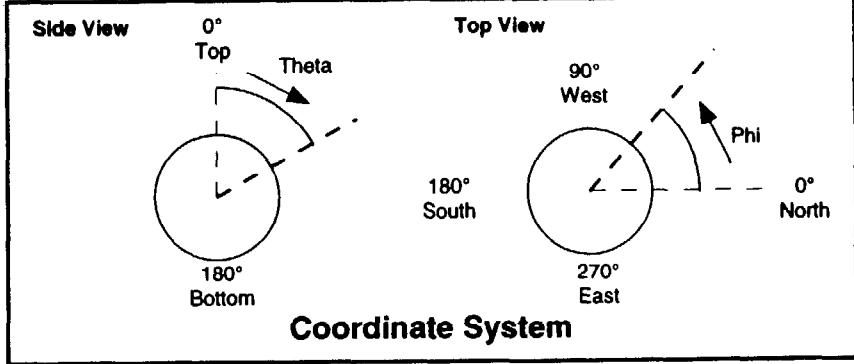
Beam 25 backscatter	1					Calorimetry only, streaking not required
Beam 30 backscatter	1					Calorimetry only, streaking not required
P510A streaks	1	Clusters 4 & 5				
Pulseshape measurements	1	Beams 19 & 20				

Note

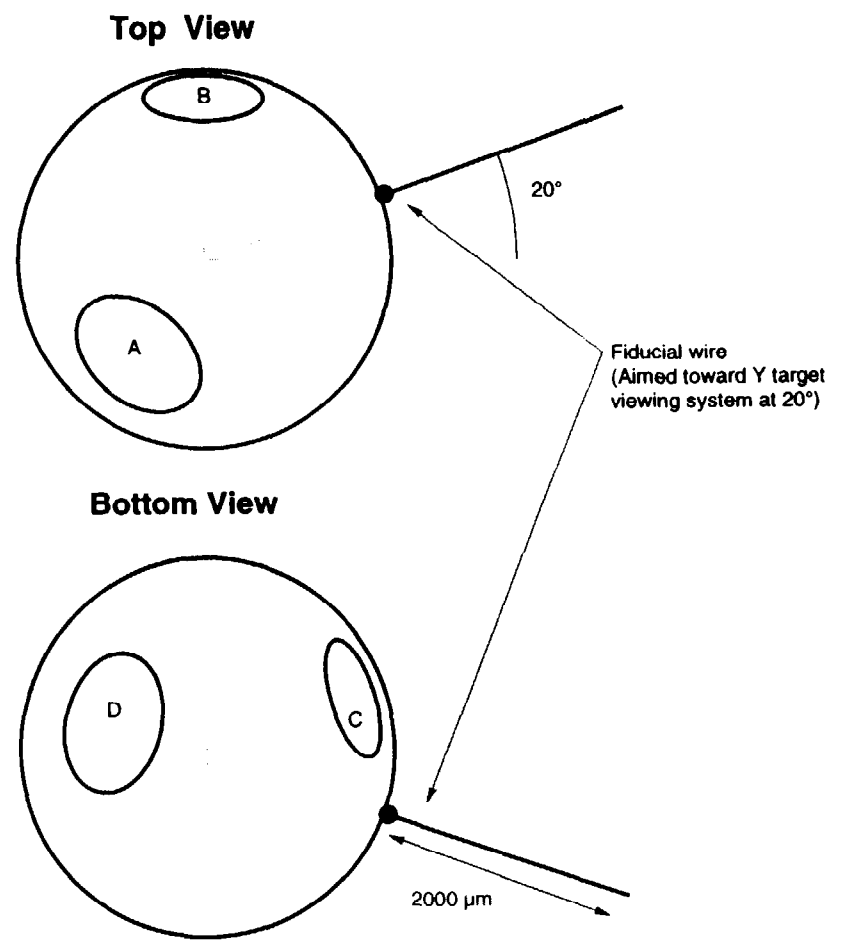
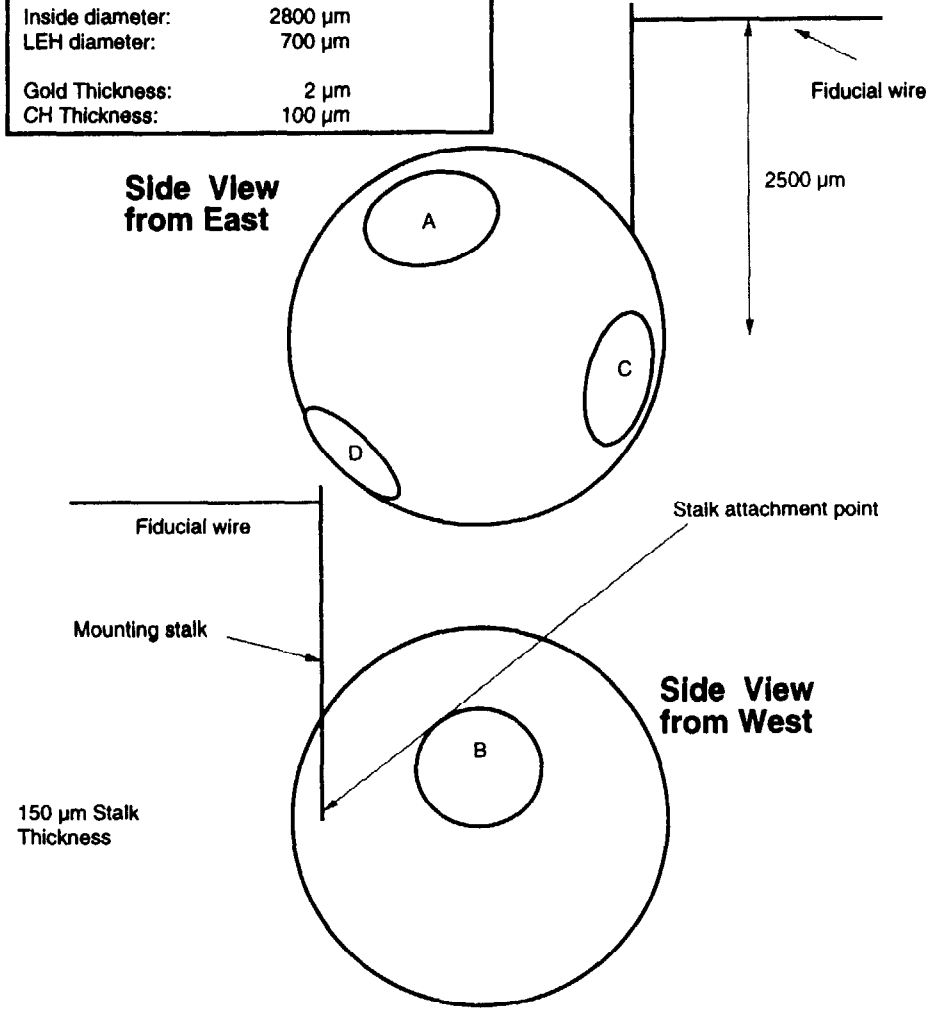
XRFC3/SXRFC should be pointed to monitor Dante Hole (LEH D), X=-808 µm, Y=-263 µm, Z=-1113 µm. All other diagnostics pointed to TCC  
 See Jon Wallace about fine tuning PS26

LEH Coordinates:		
LEH	Theta	Phi
LEH A:	37.38	234
LEH B:	79.19	90
LEH C:	100.81	342
LEH D:	142.62	198
Stalk attachment:	90.00	20
Fidu wire alignment:		20

**Tetrahedral Hohlräume for Omega**  
**H4-H7 orientation**  
**Tom Murphy**  
**July 20, 1998**  
**(not drawn to scale)**



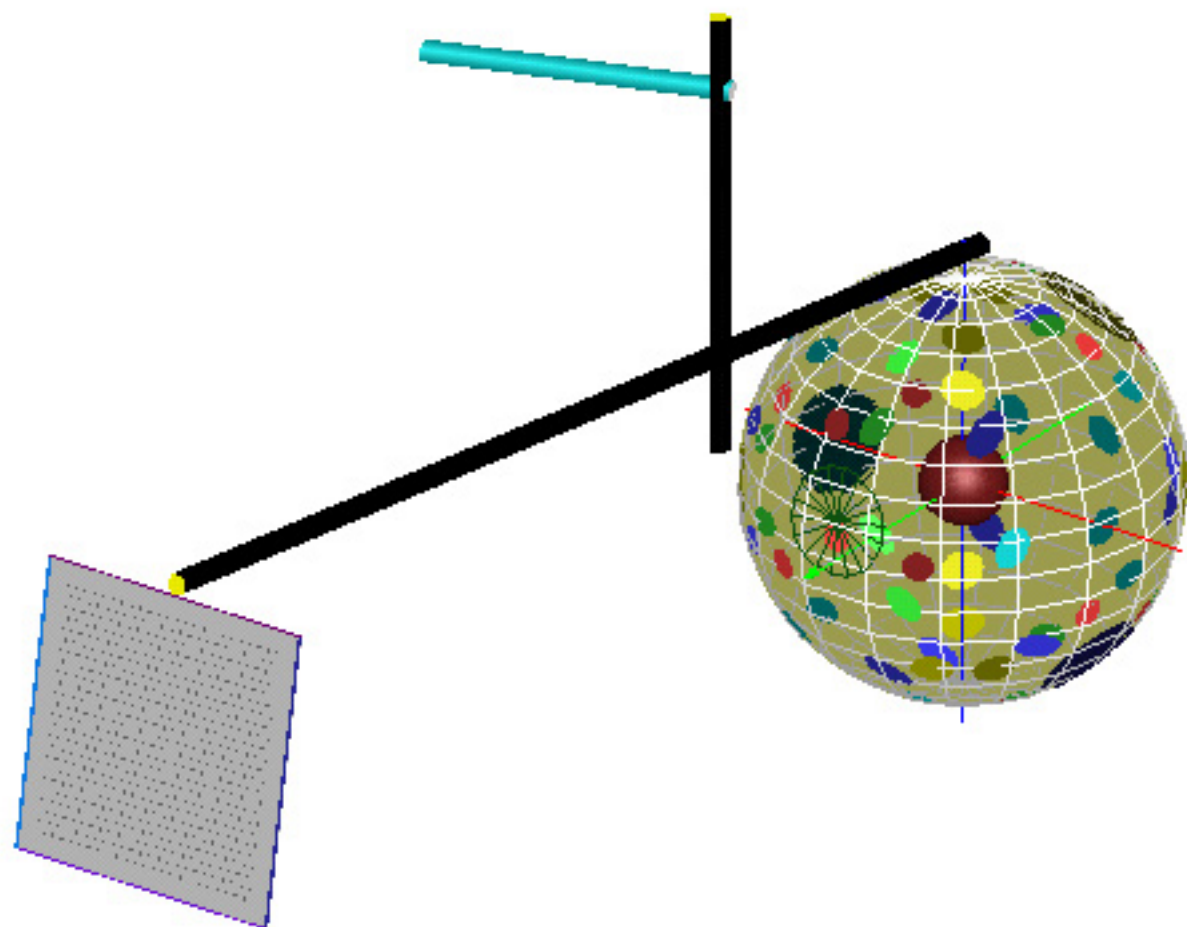
Thin-wall hohlraums	
Inside diameter:	2800 $\mu\text{m}$
LEH diameter:	700 $\mu\text{m}$
Gold Thickness:	2 $\mu\text{m}$
CH Thickness:	100 $\mu\text{m}$





**60-beam Omega Laser beam spots, Tetrahedral H4-H7**  
**Rsphere=1400 $\mu$ m, rLEH=350 $\mu$ m, Pin Array=8640 1910 sq**  
**P3    theta   63.44  $\phi$  126    -.5257 .7236 .4472 TIM#1**

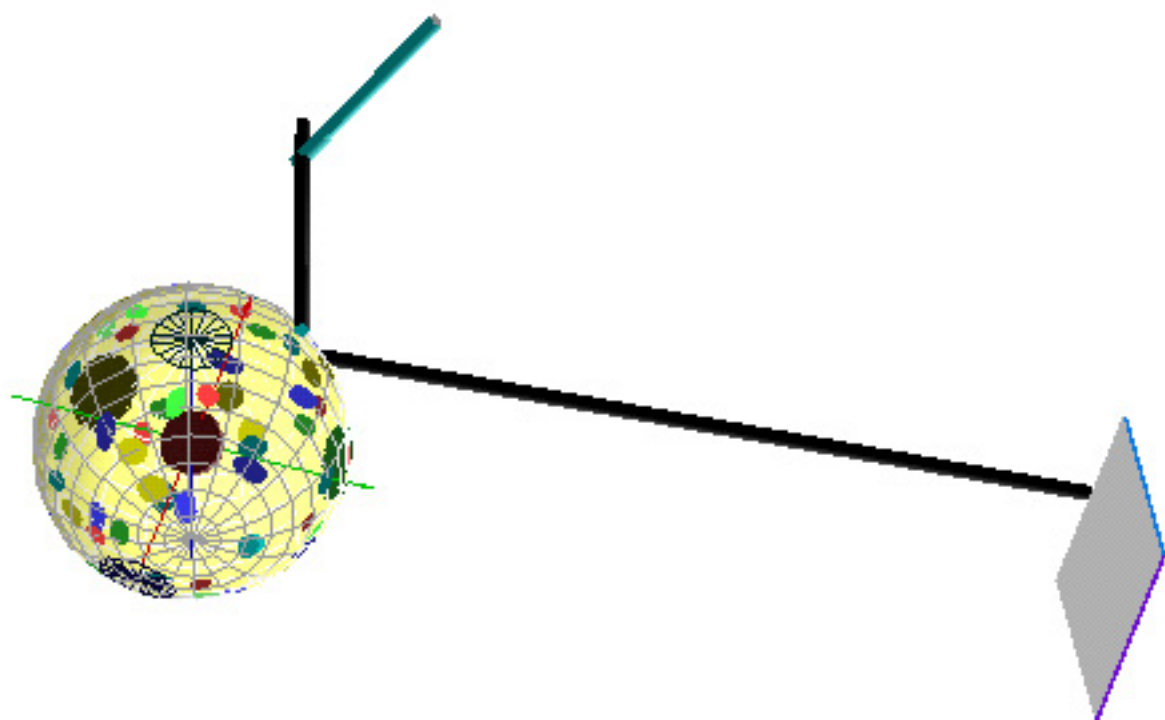
*9903spots.t3d*





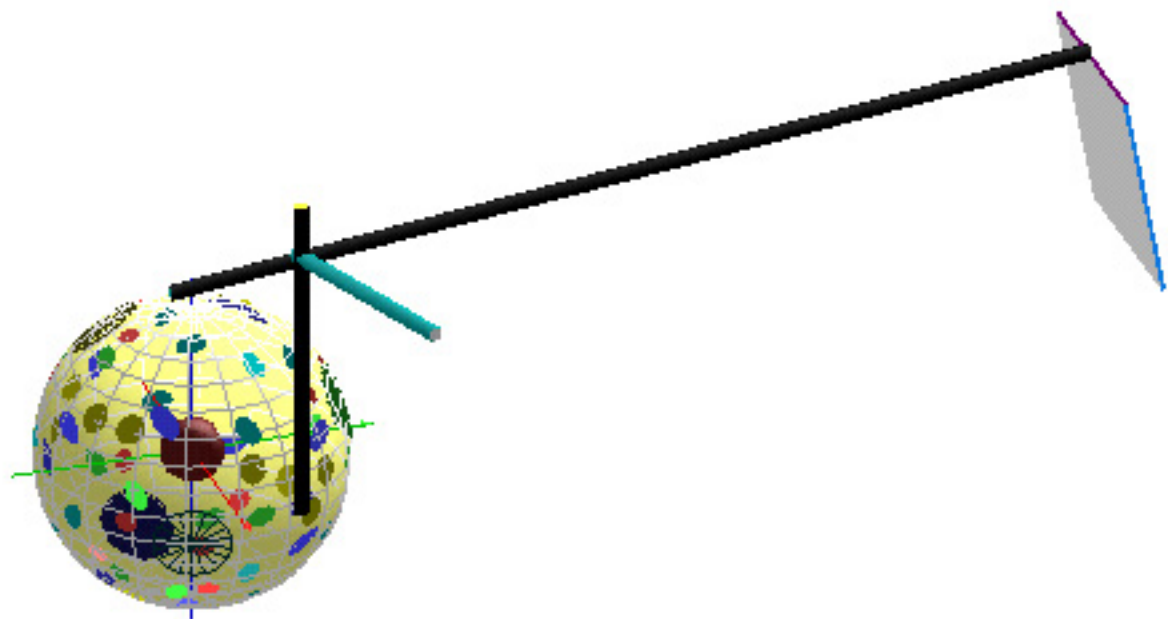
**60-beam Omega Laser beam spots, Tetrahedral H4-H7**  
**Rsphere=1400 $\mu$ m, rLEH=350 $\mu$ m, Pin Array=8640 1910 sq**  
**H18 theta 142.62  $\phi$  342 .5773 -.1876 -.7947 TIM#3**

*9903spots.t3d*



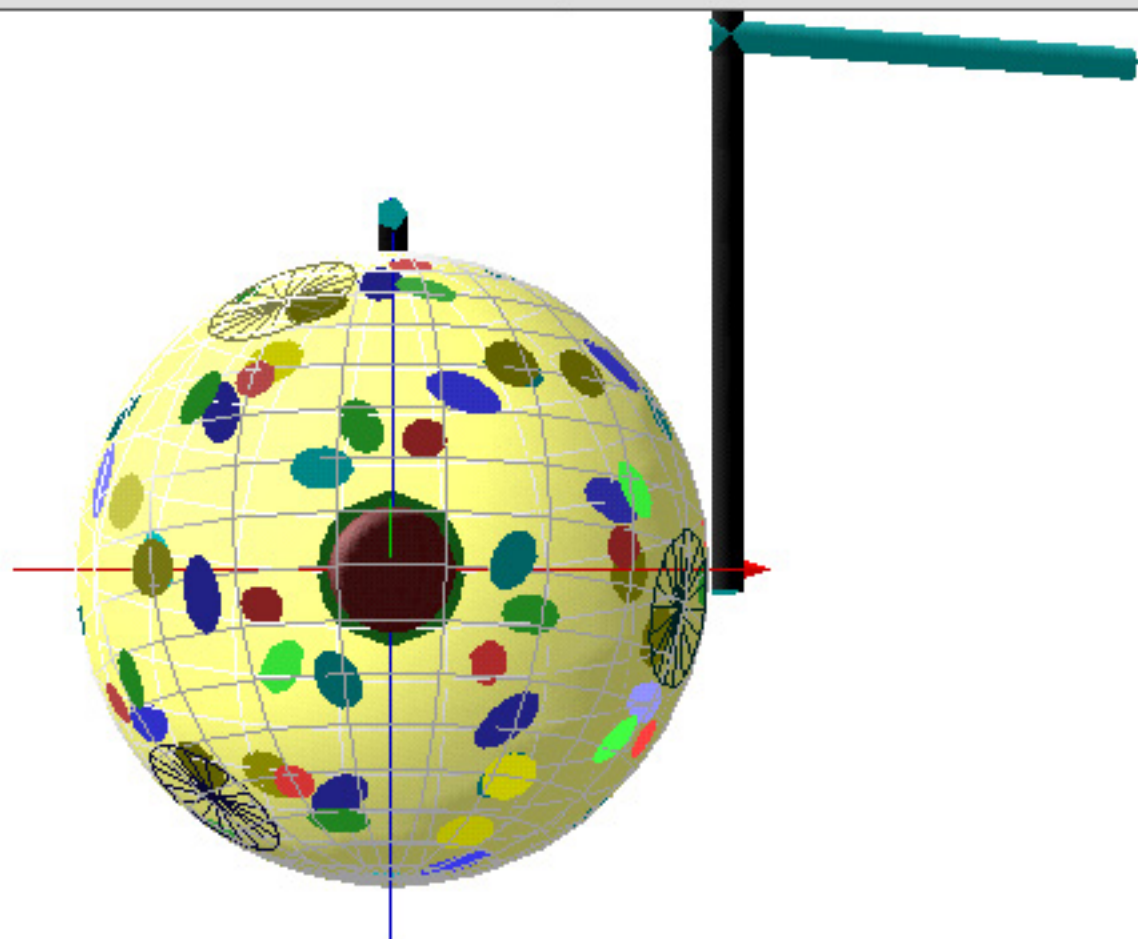
**60-beam Omega Laser beam spots, Tetrahedral H4-H7**  
**Rsphere=1400 $\mu$ m, rLEH=350 $\mu$ m, Pin Array=8640 1910 sq**  
**P6 theta 63.44  $\phi$  342 .8507 -.2764 .4472 TIM#4**

*9903spots.t3d*



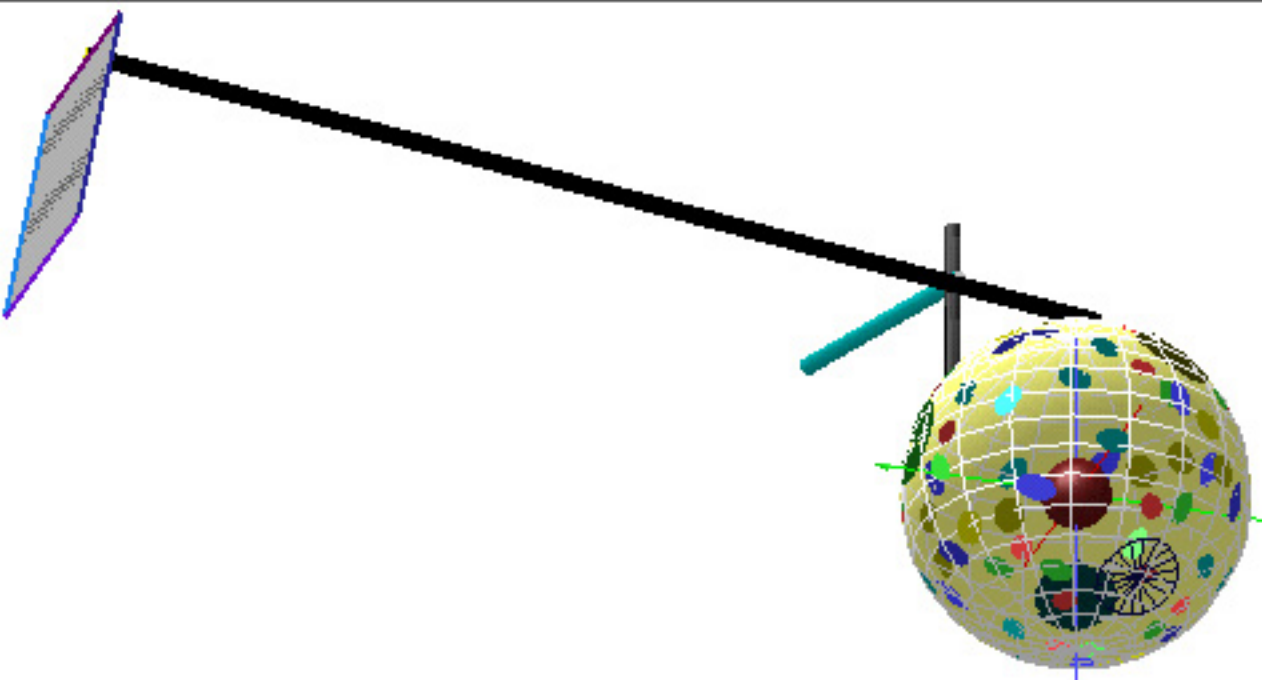
60-beam Omega Laser beam spots, Tetrahedral H4-H7  
Rsphere=1400 $\mu$ m, rLEH=350 $\mu$ m, Pin Array=8640 1910 sq  
H14 theta 100.81  $\phi$  270 .0000 -.9822 -.1876 TIM#5 SOP

9903spots.t3d



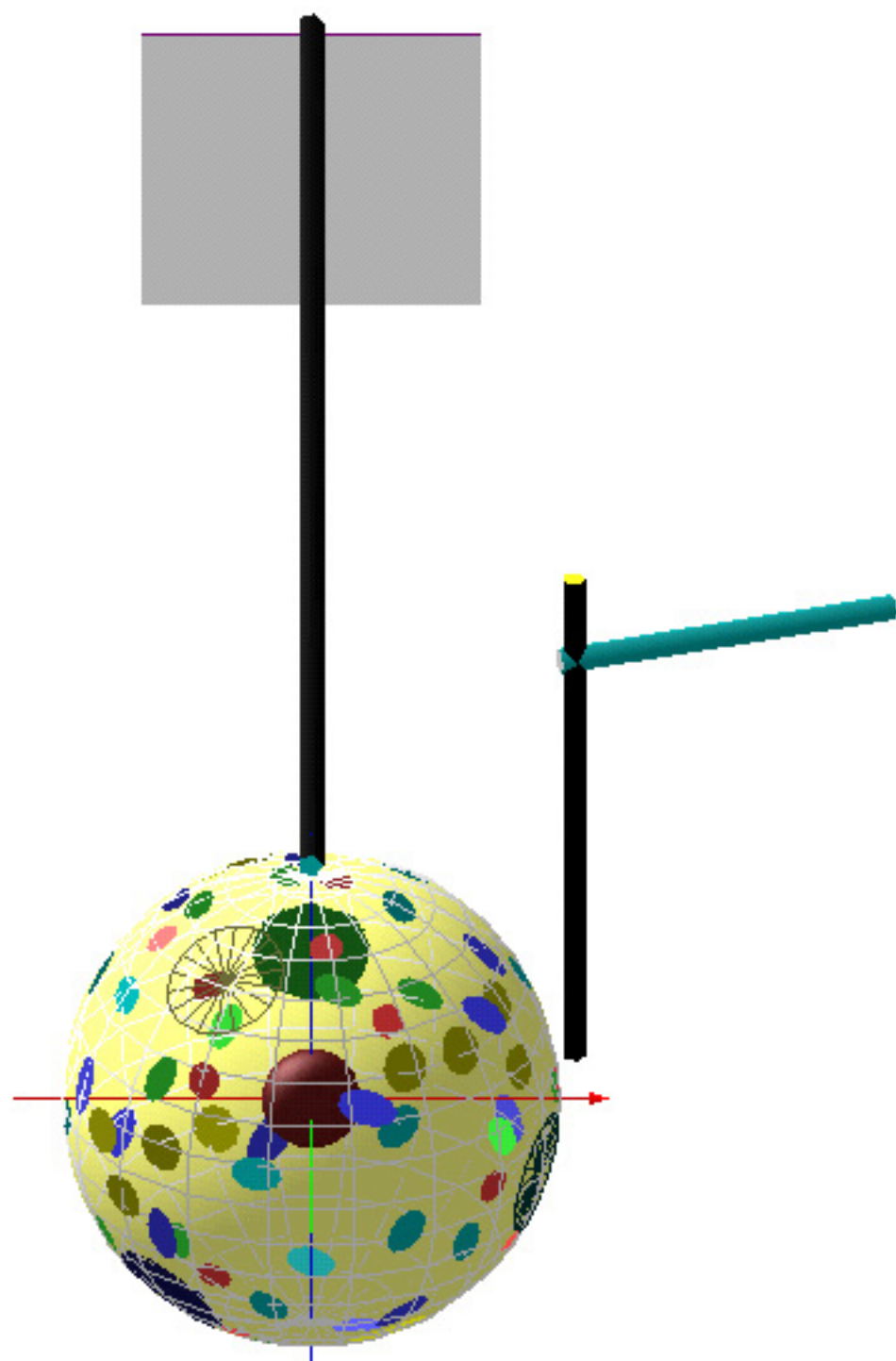
60-beam Omega Laser beam spots, Tetrahedral H4-H7  
Rsphere=1400 $\mu$ m, rLEH=350 $\mu$ m, Pin Array=8640 1910 sq  
P7 theta 116.57  $\phi$  162 -.8507 .2764 -.4472 TIM#6 cs

9903spots.t3d



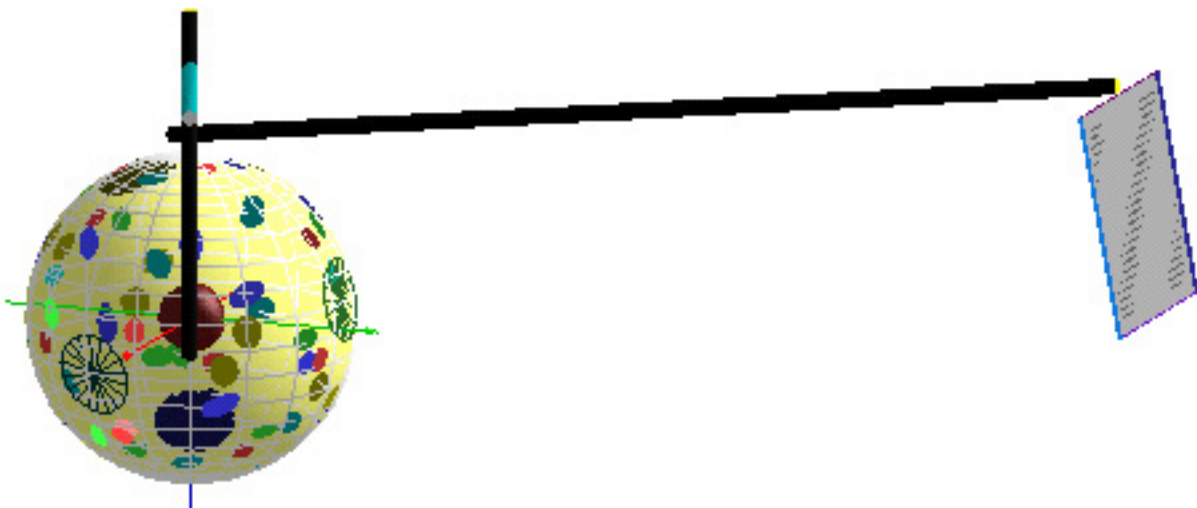
60-beam Omega Laser beam spots, Tetrahedral H4-H7  
Rsphere=1400 $\mu$ m, rLEH=350 $\mu$ m, Pin Array=8640 1910 sq  
P5 theta 63.44  $\phi$  270 .0000 -.8944 .4472 X TVS

9903spots.t3d



60-beam Omega Laser beam spots, Tetrahedral H4-H7  
Rsphere=1400 $\mu$ m, rLEH=350 $\mu$ m, Pin Array=8640 1910 sq  
H6B theta 77.28  $\phi$  19.963 .9168 .3330 .2202 Y TVS

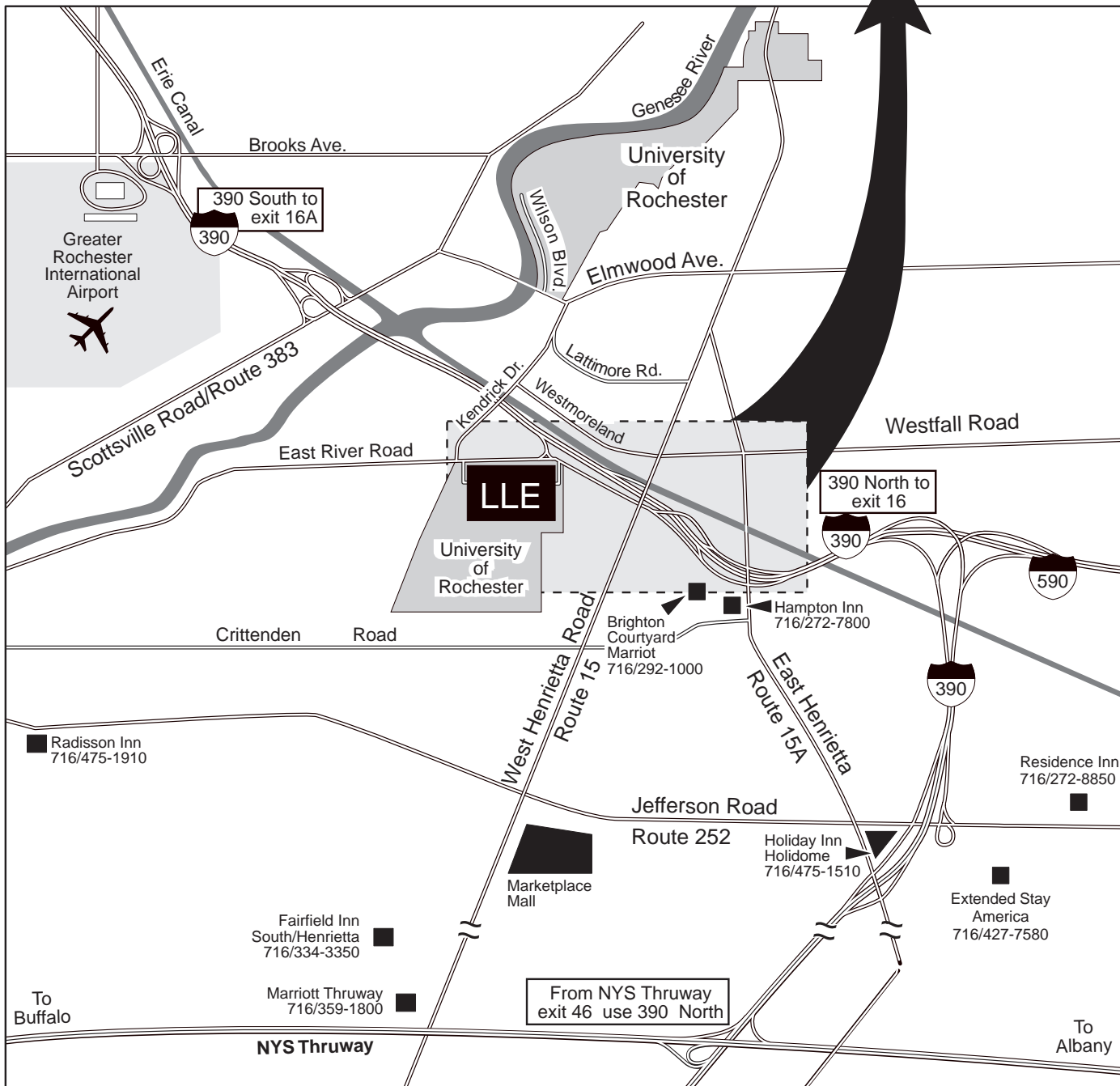
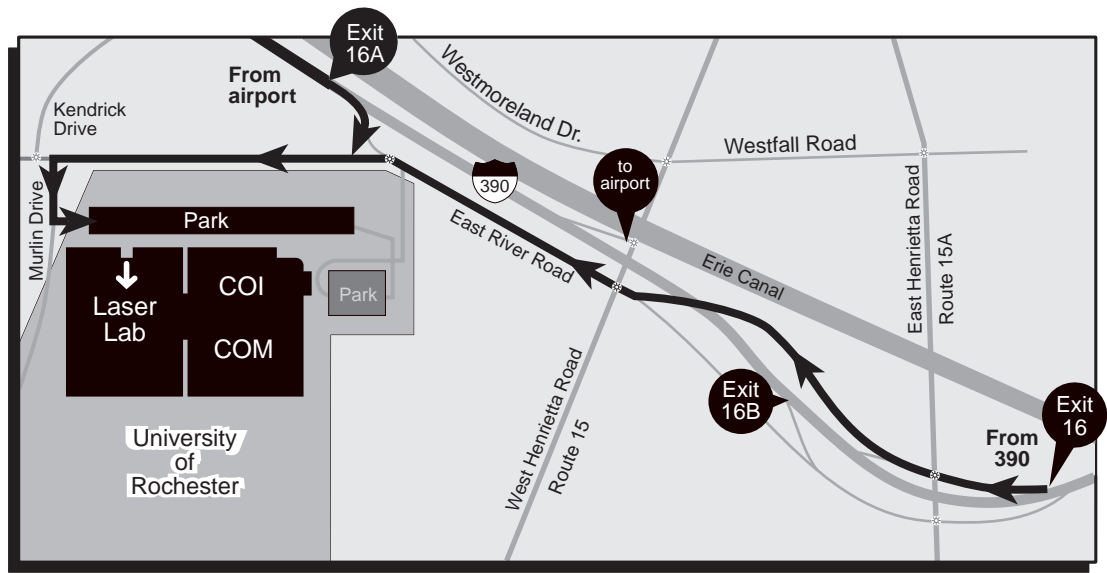
*9903spots.t3d*





# Directions to the Laboratory for Laser Energetics

250 E. River Rd.  
 Rochester, NY  
 (716) 275-5101  
 FAX (716) 275-5960



Distribution:

ID6-FY99

LANL:  T. Murphy  
 K. Klare  
 N. Delamater  
 R. Watt  
 W. Varnum  
 G. Bennett  
 J. Wallace  
 G. Kyrala  
 R. Goldman  
 J. Oertel  
 P. Walsh  
 T. Ortiz  
 T. Archuleta  
 J. Jimerson  
 A. Hauer  
 D. Wilson  
 J. Faulkner  
 L. Foreman  
 J. Fernández  
 P. Gobby  
 S. Batha  
 J. Workman  
 T. Sedillo  
 S. Evans

LLE:  R. McCrory  
 S. Loucks  
 S. Morse  
 G. Pien  
 F. Marshall  
 C. Stoekl  
 S. Craxton  
 J. Soures  
 V. Glebov  
 J. Knauer  
 N. Rogers  
 S. Skupsky  
 P. McKenty  
 D. Meyerhofer  
 T. Boehly  
 R. Keck  
 K. Thorpe  
 W. Seka

LLNL:  D. Bradley  
 S. Pollaine  
 R. Turner

Harvard:  J. Schnittman